Linear flow modelling of an integrated energy system on a national scale in 2050

Apolline Bard

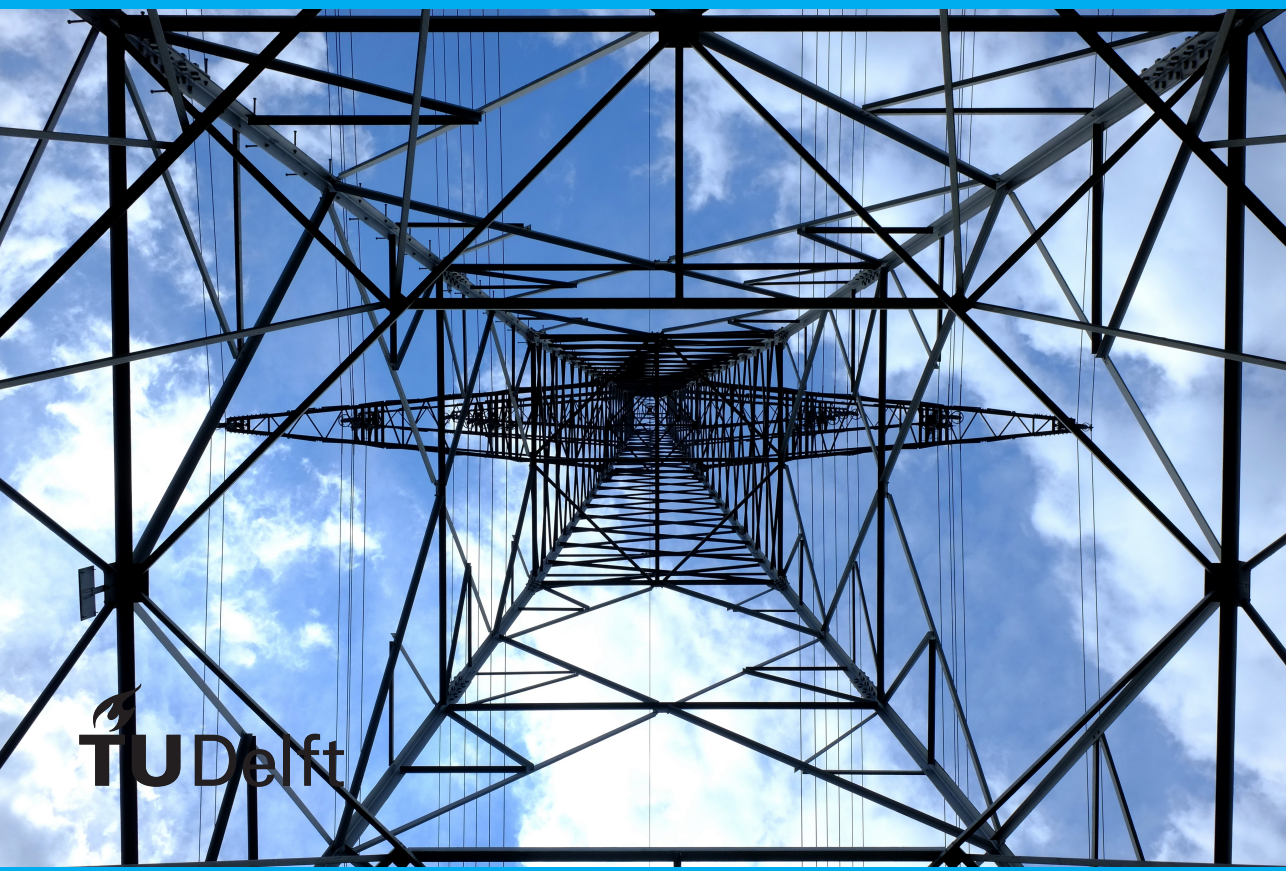

LINEAR FLOW MODELLING OF AN INTEGRATED ENERGY SYSTEM ON A NATIONAL SCALE IN 2050

by

to obtain the degree of
Master of Science
in Applied Mathematics
track Computational Science and Engineering
at Delft University of Technology,
to be defended publicly on January 7, 2022

Student number:	5137136	
Thesis committee:	Prof. Dr. Ir. C. Vuik,	Daily supervisor, TU Delft
	Dr. D.J.P. Lahaye,	TU Delft
	Dr. J.J. Steringa,	Supervisor, Gasunie
	Dr. J. van Casteren,	Supervisor, TenneT

An electronic version of this thesis is available at http://repository.tudelft.nl/.

ABSTRACT

An increasing part of European electricity is provided by renewable sources, whose output varies considerably. In order to offset these variations, gas can be used as an auxiliary source of energy for power production, but extra power can also be used to produce hydrogen or methane for storage. As a consequence, gas and power networks are growing more and more interdependent and thus need to be modelled together in order to make meaningful predictions. A growing body of literature deals with the modelling and simulation of such coupled networks, but the main focus of most sources is accuracy. On the other hand, Gasunie and TenneT's Infrastructure Outlook report aimed to study hourly snapshots of a coupled network over one year, in a variety of different scenarios. Therefore, a simplified and computationally inexpensive model was needed. Literature dealing with such models is lacking, so a linear model consisting of transport load minimization was constructed for this purpose. It was used for both gas and power simulations, but it is inadequate for the latter.

In this thesis, the transport load model is combined with the standard DC model of power flow in order to obtain more accurate results. The resulting combined linear model is tested on small sample networks, showing that it is functional given a set of modelling assumptions. In addition, the transport load model is compared to the DC model in a sample set of Dutch power networks. A large difference is observed between the two, confirming that there is no reason to use transport load as a model for electricity. Further research is needed to evaluate the accuracy of the transport load model for gas.

PREFACE

This report contains the work done for my Master's Thesis project to fulfill the graduation requirements for the MSc Applied Mathematics at the Delft University of Technology. In this project, I investigated linear models of gas and power flow based on Gasunie and TenneT's Infrastructure Outlook report. From the literature study to the final experiments, this thesis work has been demanding in whole new ways, but also an instructive and rewarding journey.

This project is exactly of the kind I was hoping to work on when I started the master program at TU Delft. I wanted to work on applied problems with a real impact, and infrastructure planning fits the bill perfectly. I was also interested in multi-disciplinary work, and this project is at the intersection of mathematics, physics and engineering. This has made it challenging, but all the more interesting. Finally, as someone with an interest in energy and sustainability, the goal of the project appealed to me. I am glad I got to write my thesis on this topic and have learned a lot in the process.

I would like to acknowledge some of the people who have supported, guided and helped me throughout this project and the writing of this report. First, I want to thank my supervisor at TU Delft, Prof. Dr. Ir. Kees Vuik, for his guidance and regular feedback. His questions and suggestions helped me push my work further and write a report I'm happy with. I also want to express my gratitude to Dr. Jarig Steringa from Gasunie and Dr. Jasper van Casteren from TenneT for making this project possible by sending me information and data, as well as patiently answering all my questions. Their input has made this project richer and extremely instructive.

Finally, I would like to thank all the people who have supported me throughout this project and during my studies at TU Delft: my parents for the everyday support and for making sure I got out of the house; Kannan for the accountability checks and constant encouragement; and lastly, Dario, Yimin, Franco, Diego and Shashank for being my TU Delft family. I can never thank you enough for showing me where I belong.

Delft, December 2021

CONTENTS

List of Figures

1

INTRODUCTION

An increasing part of European energy is provided by renewable sources such as wind and solar. They have the major advantage of being more sustainable than fossil fuels, but they come with their own constraints. Indeed, the energy they provide fluctuates depending on the weather conditions [1]. On the other hand, in power networks, supply and demand must be balanced for stability [2]. This means that ways must be found to absorb the excess renewable energy when supply exceeds demand, and to inject extra energy into the network when supply is insufficient. Gas-fired power plants can provide the latter [3]; more recently, power-to-gas technology has been studied as a way to store surplus renewable electricity in the form of hydrogen or synthetic methane [4]. This connection of two energy networks is called sector coupling.

The use of these technologies implies that power and gas networks are becoming increasingly interdependent. Thus, it is useful to model them together, be it for day-to-day dispatch of energy sources or for long-term infrastructure planning. In the Infrastructure Outlook 2050 [5], Gasunie and TenneT studied different scenarios for the evolution of energy infrastructures: power grid, natural gas network and hydrogen network. The idea was to obtain hourly snapshots of supply and demand over an entire year. This represents 8760 individual calculations, so a computationally inexpensive model was needed. A linear model based on the transport moment (transport load model) was used for all three component networks. While it was sufficient to get a general idea of the gas networks' behaviour, it proved inaccurate for electricity because it did not correctly reflect the physics of the power network.

The object of this thesis is to construct, evaluate and apply an improved model for the combined network. This model needs to make physical sense, but we are also looking to keep it simple. The goal is therefore to construct a linear optimization problem which combines transport load of gas and standard linear models of power flow, while preserving accurate communication between component networks. This model is tested on a set of example networks. Finally, it is applied to the study of a simplified version of the anticipated Dutch combined network. As in the Infrastructure Outlook report, the results are used to provide a binary answer to the question: *Is this network configuration*

viable?

The rest of this document is organized as follows. First, the literature review examines some of the literature of multi-carrier energy networks. The next section details the construction of the combined model and the procedure used to compare it to the transport load model. Then, the results obtained with the combined model are examined, both for the test network and the future Dutch network under investigation. Finally, the results are discussed and put into perspective.

2

LITERATURE REVIEW

THe study of multi-carrier energy systems is a relatively recent field. Its foundational papers were written in the early 2000s and include, for example, [3], [6]. All of them studied natural gas networks and power networks with gas-fired power plants; models including power-to-gas came later. In 2007, [7] introduced the concept of energy hub as a way to couple general multi-carrier energy systems. Since then, many other papers have been written and various aspects of the problem studied. These aspects range from pure network modelling to infrastructure and market planning. In this chapter, we review some literature dealing with coupled power and gas networks.

2.1. COMPONENTS OF COUPLED NETWORKS

For both the power and gas components, the network is represented with nodes and lines. At nodes, mass or energy conservation is enforced; in lines, specific equations describe the flow in terms of the conditions at the source and target nodes of the line.

2.1.1. POWER NETWORKS

In power networks, energy conservation at nodes is stated by Kirchhoff's current law (KCL): the sum of currents entering a node (or bus) must equal the sum of currents leaving it. This may be written in several different ways: in complex form [7] or with separate equations for active and reactive power [3]; as one equation per bus [8] or as a sum over the whole network [9]. For example, in complex power form, KCL for a single bus j reads

$$P_j - \sum_{i \neq j} P_{ij} = 0,$$

where P_j is the power injected at bus j and P_{ij} is the power flowing between buses i and j. For the whole network, assuming that all losses are modelled as bus power injections, it is written as a sum over all nodes j:

$$\sum_j S_j^{\text{source}} = \sum_j S_j^{\text{load}}.$$

As for the power flow in lines, it can be represented in two ways. High-voltage power networks use alternating current (AC), which is represented with nonlinear equations: the active power flowing in line ij is given by

$$P_{ij} = V_i V_j \frac{\sin(\delta_i - \delta_j)}{x_{ij}}.$$

Under the assumptions that all voltages V have unit value and that the angle differences $(\delta_i - \delta_j)$ are small, this can be simplified into a linear approximation called DC power flow:

$$P_{ij} = \frac{\delta_i - \delta_j}{x_{ij}} = b_{ij}(\delta_i - \delta_j).$$

Both linear and nonlinear equations are used throughout the literature. AC equations are more accurate, but solutions are more difficult and more expensive to compute due to their nonlinearity. They are thus used in papers where the authors are after higher accuracy: for instance, in short-term scheduling of energy networks. On the other hand, DC equations are widely used because they are easy to solve. In order to avoid dealing with voltage angles, they are rewritten in terms of power transfer distribution factors (PTDF). Using the PTDF matrix (as explained in [10]), the flow in line ij given by:

$$P_{ij} = \sum_m \text{PTDF}_{ij,m} P_m$$

In a full power network model, nodal equations and flow equations are used along with various constraints on line capacity, generator capacity, power demand, bus voltage, etc.

Finally, the Infrastructure Outlook report [5] uses the transport load model (see chapter 3 for its construction) for the power network as well as the gas network. However, this does not correctly reflect the physics of the power network because changes in the power network are instantaneous, while transport load is more suited for a medium that moves at slow speeds, such as gas.

2.1.2. GAS NETWORKS

In all the papers considered, the gas component of the combined network contains natural gas. Only the Infrastructure Outlook [5] uses both a hydrogen and a gas network, and it is also the only one using a linear model. This model was initially developed by [11].

In gas network models, mass conservation is enforced at every node. As for the gas flow in pipes, all the papers studied use a variant of the same gas flow equation,

$$q_{ij} = C_{ij} \sqrt{p_i^2 - p_j^2}.$$

The steady-state gas flow in pipeline ij is thus a quadratic function of the pressures at its end nodes, p_i and p_j. The direction of the flow is always from high to low pressure. The coefficient C_{ij}, called *pipe conductivity*, depends on the choice of equation. A number of possibilities are given in [12]. This coefficient can depend on such factors as pipeline efficiency, gas gravity, pipe length, pipe diameter, gas compressibility factor,

etc. Additional parameters are sometimes used: for instance, [8], [13] take into account the change of elevation in the pipeline.

This flow equation is nonlinear and nonconvex, which makes solving gas flow problems complex and computationally expensive. Some papers such as [14], [15] present clever ways to solve them iteratively, but the fundamental equations are still the same. This is why having a linear model is interesting: even though it is a rough approximation, it allows us to easily get a general idea of flow patterns in the network. In particular, since we are looking to decide whether or not a particular network configuration is feasible, this approximation is interesting.

2.2. COMMUNICATION BETWEEN COMPONENT NETWORKS

Constructing a model for a combined gas and electricity network involves an exchange of information between the two. This most often occurs through a coupling node, a point in the network which involves both forms of energy. In this section, we take a brief tour through the types of coupling nodes used in the literature.

2.2.1. GAS-FIRED GENERATORS

Gas-fired power plants, or generators (GFG), are the type of coupling node found in the earliest literature (see [3], [16]). As they are used to offset daily variations in electricity demand, the volume of gas consumed is modelled as a function of the power output needed, P_g. In a detailed model, the energy demanded by a GFG with index i is given by its heat rate curve,

$$\mathrm{HR}(P_g) = \alpha_i + \beta_i P_g + \gamma_i P_g^2$$

where both P_g (the power output needed in the network) and HR are in MW. The volume of gas consumed then depends on its heating value HV. This may be the higher heating value (HHV) or the lower heating value (LHV), depending on the modelling assumptions and the goal of the model. The volume of gas consumed is given by

$$G_{\mathrm{gfg}} = \mathrm{HR}(P_g)/\mathrm{HV} = (\alpha_i + \beta_i P_g + \gamma_i P_g^2)/\mathrm{HV}.$$

Here we have HR in MW and HV in MW$\cdot$ m^{-3}, so G_{gfg} is given in m^3.

Another option is to use a linear relation, as in [5], [9]: an efficiency coefficient η_{gfg} is used and the power output is given as

$$P_g = \eta_{\mathrm{gfg}} \cdot G_{\mathrm{gfg}} \tag{2.1}$$

2.2.2. POWER-TO-GAS PLANTS

Power-to-gas technology consists of using electricity to produce hydrogen through electrolysis, or synthetic natural gas (SNG) through methanation of the previously obtained hydrogen [17]. It allows for surplus renewable electricity to be stored on the short or long term. Compared to SNG, hydrogen has the advantage of causing less energy loss upon conversion: producing hydrogen using electricity then combusting the resulting hydrogen (round trip) produces 34-44% of the initial amount of electric energy, while the round-trip efficiency for synthetic methane is 30-38% [4]. Both SNG and hydrogen are entirely compatible with the existing high-pressure natural gas infrastructure, at least

in the Netherlands [18]. Mixtures are acceptable as well, though mixing of natural gas and hydrogen is considered a short term solution and is not foreseen for the longer term (2050) in the Dutch energy system.

Since power-to-gas technologies are only starting to become economically viable [1], all the sources for this part (e.g. [9], [17], [19], [20]) are very recent. All of them use a linear relationship for power-to-gas modelling. The volume of gas obtained is thus represented by

$$G_{\text{p2g}} = \eta_{\text{p2g}} \cdot P_l / \text{HV} \tag{2.2}$$

where P_l is the power load of the P2G facility. As before, HV is in MW$\cdot$ m^{-3} and P_l is in MW. The efficiency coefficient η_{p2g} is unitless and G_{p2g} is thus given in m^3.

This relationship has the same form whether the gas in question is hydrogen or methane, though the efficiency and heating value are not the same. Indeed, hydrogen has a lower heating value than methane and thus a larger volume is necessary to obtain the same amount of power.

2.2.3. COMPRESSOR STATIONS

Compressor stations may be powered by electricity, as in [7], [9]; in that case, they act as a coupling node between the gas and the electricity networks. The energy they consume is then converted into a load on the electricity network. Compressors can also be gas-powered (see for example [3]), but in this case they are not a point of coupling.

2.2.4. ENERGY HUBS

Energy hubs are occasionally used for general multi-carrier energy systems. They are an interesting way to represent systems with more than 2 energy carriers. They were first introduced by [7] and they serve to represent a set of energy exchanges: an energy hub may contain sources, loads, converter devices, and storage facilities. The system is then represented as a network of energy hubs. Converter devices are represented with a coupling efficiency between each energy carrier. This efficiency may or may not be linear.

2.3. SOLVING STRATEGIES

A range of solving strategies are used in the literature of combined energy networks. In fact, quite often, they are the central part of the paper since the models under study are difficult and computationally expensive to solve.

2.3.1. OPTIMIZATION MODELS

An underdetermined system of equations is obtained from all the governing equations listed above. Constraints are put on each component of the network (some are listed throughout the previous sections). The objective function is often the fuel cost (to be minimized), but other choices are possible [7], [21], such as throughput maximization, profit maximization, loss minimization, or pollution minimization. In general, the system is nonlinear and nonconvex due to the gas flow equations. A variety of strategies are thus used to compute the optimal solution, such as piecewise linearization [22] or specific nonlinear optimization solvers.

On the other hand, the Infrastructure Outlook uses the linearized model of [11]. The cost functions and constraints are therefore entirely linear and linear optimization can be used. This is the case in this project as well.

2.3.2. SOLVING WITHOUT OPTIMIZATION

After combining the elements of the network, it remains to solve a system of equations: power flow, power balance at nodes, gas flow, gas balance at nodes, coupling node equations. This is generally a system of nonlinear equations which cannot be solved analytically, hence the use of numerical methods. This strategy is used in [8], [13], [23]. The system of equations is generally undetermined. An initial guess is provided by the user, which contains enough data to ensure that the solution based on that guess is unique. However, it is not necessarily optimal [21]. In addition, finding a reasonable value for such a guess is challenging.

2.4. CASE STUDIES AND AVAILABILITY OF REFERENCE DATA

All of the papers studied come with at least one case study demonstrating the functioning of the model presented. Since that is also an important part of this thesis, it is instructive to look at how such examples are chosen.

2.4.1. POWER NETWORKS

Standard IEEE test cases are used as the power network in case studies throughout the literature. They are well-studied and have readily available solutions, which can for instance be computed using the MATPOWER library [24]. However, one drawback for this project is that many do not have linear generator costs. This means they cannot be used within a linear optimization problem without modification.

2.4.2. GAS NETWORKS

There is no standard for test cases of gas networks, so the papers studied here use many different ones. A variety of small networks are thus used; the only reoccurring one is a model of the Belgian gas network [8], [9], [16], since the data for this one is publicly available. A library of gas networks has also recently been collected [25] under the name GasLib; it contains some small networks for testing purposes as well as some large ones based on real-world data. However, solution data are lacking, which makes comparison difficult.

2.4.3. COMBINED NETWORKS

In order to construct a combined network, a gas network is coupled to a power network at one or more points. The resulting power and gas flows are different from those obtained in decoupled network. Thus, input data are often available, but complete solution data are much more difficult to find; of the papers reviewed in this chapter, only [13] provides a full solution. This makes it challenging to compare the solutions obtained in this work to solutions obtained with other models.

2.5. DISCUSSION AND CONCLUSION

We have explored multiple ways to formulate and solve steady-state flow problems in combined gas and electricity networks. The goal of the project is to formulate a linear model; however, it is instructive to look at more elaborate ones, as they offer insight into the challenges of network modelling. Many authors focus on aspects which are not directly relevant for this project, such as day-to-day scheduling or market planning. For this reason, they need high-accuracy models, and linear ones are not suitable for their purposes. On the other hand, this project will focus on the feasibility of scenarios for future infrastructure, and thus a first-order approximation is sufficient for now. In any case, care must be taken to state the simplifying assumptions clearly and to construct a reasonable linearization. For power flow, there is a single standard linear model, but this is not the case for gas flow. As for interaction between networks, each component can be described with a linear model or a constant, but so far we have no description of how to calculate the parameters involved. Finally, a range of solving strategies has been described; they depend in part on the model formulation, but also on the desired numerical properties.

3

A LINEAR MODEL FOR COMBINED GAS AND POWER NETWORKS

In this section, we put together a linear model for a coupled energy network by using together the DC power flow model and the transport load model. We first present the components separately, then show how to combine them.

3.1. POWER FLOW

For this part, we use the DC approximation of power flow mentioned in chapter 2. This is a standard, widely accepted model.

3.1.1. PRINCIPLES

Optimal power flow (OPF) consists of computing the optimal way to generate power given the demand. In this thesis, the DC model is used: the resulting linear optimization problem is called DC OPF. The costs here are generation costs: each power plant has an associated cost. The idea, then, is to make the power supply match the load in the cheapest possible way. A trivial way to do this would be to make the cheapest generator produce all the power, but two things prevent us from doing this. First, generators can only produce so much power: they have a capacity limit. There may also be a lower bound on their energy production, as depending on the nature of the power plant, stopping production entirely can be complicated. The second factor is the capacity of the power lines; they too have physical limits and cannot carry an unlimited amount of power.

3.1.2. DC OPTIMAL POWER FLOW

For this problem, the optimization variable is the vector of generated power, $\mathbf{P}_G$, where the i-th entry represents the power generated at bus i. The cost vector $\mathbf{c}$ similarly gives the cost of each generator, and so we are looking to minimize the linear cost function:

$$\min \mathbf{c}^\top \mathbf{P}_G \tag{3.1}$$

This is subject to a set of constraints, the first of which is the capacity of the generators:

$$P_{G_i}^{\min} \leq P_{G_i} \leq P_{G_i}^{\max} \quad \text{for each } i \tag{3.2}$$

The second constraint is energy conservation: the supply P_G should match the demand P_D. This is given over the whole network:

$$\sum_i P_{G_i} = \sum_i P_{D_i} \tag{3.3}$$

Finally, we consider the line capacity limits: the power flowing in each line must be smaller than or equal to the capacity of that line. This is where we use the PTDF matrix to easily compute the flow in each line. (See appendix A for an explanation of how this matrix is obtained.) Since power can flow in either direction in a line, we have two inequality constraints for each line:

$$-\mathbf{P}_{\text{line}}^{\max} \leq \text{PTDF} \cdot (\mathbf{P}_G - \mathbf{P}_D) \leq \mathbf{P}_{\text{line}}^{\max} \tag{3.4}$$

Note that not all lines need to have specified capacity limits; for example, in the 5-node network which is used later as a test case, only two such limits are given. In that case, only the corresponding rows of the PTDF matrix are included in the calculation.

Putting everything together, the DC OPF problem is as follows:

$$\begin{aligned} & \min \sum_i c_i P_{G_i} \\ \text{subject to} \quad & P_{G_i}^{\min} \leq P_{G_i} \leq P_{G_i}^{\max} \\ & \sum_i P_{G_i} - \sum_i P_{D_i} = 0 \\ & -\mathbf{P}_{\text{line}}^{\max} \leq \text{PTDF}\,(\mathbf{P}_G - \mathbf{P}_D) \leq \mathbf{P}_{\text{line}}^{\max} \end{aligned} \tag{3.5}$$

This problem formulation is used for the test networks presented in chapter 4. For the Dutch network instances, the case data (provided by Gasunie) includes previously optimized values for generated power, so this step is skipped.

3.2. GAS FLOW

The model used for gas flow is the transport load. It is defined as the product of the distance covered L and the quantity transported Q:

$$T(Q) = LQ \tag{3.6}$$

The sum of this quantity over all pipelines in the network is minimized.

3.2.1. PRINCIPLES

The standard gas flow equations described in chapter 2 are nonlinear and nonconvex, leading to optimization problems that are complex and expensive to solve. Instead, the linear approximation constructed in [11] is used. The driving force is still the pressure differential: gas moves from high to low pressure. Because of friction against the pipe

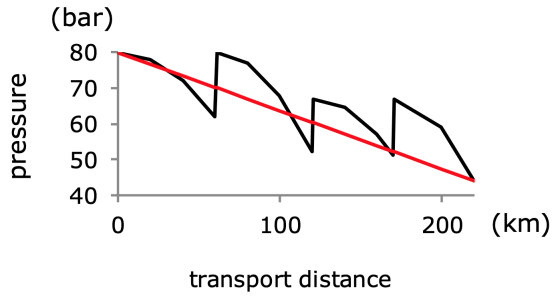

Figure 3.1: Pressure decrease for transport of gas in a network with intermediate compression (black line) and its linearization (red line)

walls, a loss of power occurs, which can be written in terms of the pressure difference $\Delta p = p_{\text{in}} - p_{\text{out}}$ and transported quantity of gas:

$$\Delta P = Q\Delta p.$$

Now, pressure decreases with distance, and the pressure profile along a pipe is generally nonlinear. This is particularly true when a pipe contains compressors, which gives a sawtooth-shaped profile. The idea is to approximate this profile with a linear function, as illustrated by fig. 3.1. The pressure difference can then be approximated as a linear function of the distance, $\Delta p \propto \Delta L$ for some coefficient a.

The loss of power for a given distance then becomes

$$\Delta P \propto Q\Delta L$$

so over the whole line, we have

$$P \propto QL.$$

Notice that the right-hand side is the same as the RHS of eq. (3.6), i.e., the transport load. By minimizing the transport load, the idea is thus to minimize the losses of power over the network.

In practice, the actual transport load function is defined piecewise since the transported quantity has a sign (positive in one direction of transport, negative in the other). The capacity of the line is also not necessarily the same in either direction. Additionally, the capacity is not a hard limit; rather, it is used as a threshold above which the cost is much higher. This allows the optimization to be feasible even when the network is congested, while keeping the same optimal values for the optimization variables. For each pipeline k, the transport load function T_k is defined as follows:

$$T_k(Q_k) = \begin{cases} -NL_kQ_k, & Q_k < Q_k^{\min} \\ -L_kQ_k, & Q_k^{\min} \le Q_k < 0 \\ L_kQ_k, & 0 \le Q_k \le Q_k^{\max} \\ NL_kQ_k, & Q_k > Q_k^{\max} \end{cases} \tag{3.7}$$

where N is a large number which serves to penalize flows larger than the line capacity. This is illustrated by fig. 3.2.

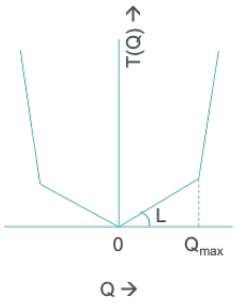

Figure 3.2: Piecewise linear load function of a line of length L

3.2.2. TRANSPORT LOAD OPTIMIZATION

The sum of the transport load in each pipe is minimized, subject to mass conservation at each node: the total amount of gas arriving at the node and leaving it must be the same. This includes the signed gas quantities and the external gas injection at that node, w_i. The construction of an equivalent linear problem out of a piecewise linear one is explained in appendix C. The optimization problem is then:

$$\begin{aligned} &\min \sum_k T_k(Q_k) \\ \text{subject to} \quad &w_i = \sum_j Q_{ij} \quad \text{for each } i \end{aligned} \tag{3.8}$$

Here $Q_k = Q_{ij}$ is the gas load in pipe k joining nodes i and j.

Contrary to DC power flow, this is not a standard model. In the next chapter, we see that it gives a rough approximation of gas flows. However, it is useful for obtaining a general idea of flow behaviour.

3.3. ENERGY CONVERSION

Energy conversion is modeled with a linear relationship. Each conversion has an efficiency factor η.

3.3.1. GAS TO POWER

A gas-fired generator j (part of the power network) is associated with a node i of the gas network. This node exclusively provides all the gas required by the generator at j; in other words, all the gas leaving node i is used at j, and this is the only source of energy for that generator. Therefore, the power generated at node j is $P_j = \eta_{\text{gfg}} w_i$. This means the gas balance equation at i is now

$$\sum_k Q_{ik} - \frac{1}{\eta_{\text{gfg}}} P_j = 0. \tag{3.9}$$

3.3.2. POWER TO GAS

In the same way as before, we assume that the entirety of the gas supply at the target node G_j is provided by power leaving the source node P_i, and that all the power leaving P_i is used for that purpose. This means the gas injection at G_j is

$$w_j = \eta_{\text{p2g}} P_{D_i}. \tag{3.10}$$

3.4. COMBINED OPTIMIZATION PROBLEM

We can now assemble the components described in the previous sections. Without coupling, the combined problem is given by:

$$\begin{aligned} \min \sum_k T_k(Q_k) + \sum_i c_i P_{G_i} \\ \text{subject to} \quad & P_{G_i}^{\min} \le P_{G_i} \le P_{G_i}^{\max} \\ & \sum_i P_{G_i} = \sum_i P_{D_i} \\ & w_i = \sum_j Q_{ij} \\ & -\mathbf{P}_{\text{line}}^{\max} \le \text{PTDF}\,(\mathbf{P}_G - \mathbf{P}_D) \le \mathbf{P}_{\text{line}}^{\max} \end{aligned} \tag{3.11}$$

Putting the equality constraints in matrix form and rearranging the last line:

$$\begin{aligned} \min \sum_k T_k(Q_k) + \sum_i c_i P_{G_i} \\ \text{subject to} \quad & P_{G_i}^{\min} \le P_{G_i} \le P_{G_i}^{\max} \\ & \mathbf{1}^\top \mathbf{P}_G = \sum_i P_{D_i} \\ & M\mathbf{Q} = \mathbf{w} \\ & \text{PTDF} \cdot \mathbf{P}_G \le \mathbf{P}_{\text{line}}^{\max} + \text{PTDF} \cdot \mathbf{P}_D \\ & -\text{PTDF} \cdot \mathbf{P}_G \le \mathbf{P}_{\text{line}}^{\max} - \text{PTDF} \cdot \mathbf{P}_D \end{aligned} \tag{3.12}$$

where M is the negative of the branch-node incidence matrix of the network graph and $\mathbf{1}$ is the column vector of ones. This means if we put all the variables in a single vector, the matrix A_{eq} representing the inequality constraints is block diagonal:

$$\begin{pmatrix} \mathbf{1}^\top & 0 \\ 0 & M \end{pmatrix} \begin{pmatrix} \mathbf{P}_G \\ \mathbf{Q} \end{pmatrix} = \begin{pmatrix} \sum_i P_{D_i} \\ \mathbf{w} \end{pmatrix} \tag{3.13}$$

It is in the bottom left block of A_{eq} that we make modifications to account for the coupling links. First, take the gas-fired generator modeled by eq. (3.9). In practice, we need to modify the row corresponding to the i-th gas node, which is row $i+1$ of the matrix equation eq. (3.13). We set w_i (the RHS) to 0 and the entry corresponding to P_j (the j-th column) to $1/\eta_{\text{gfg}}$.

Next, we add in eq. (3.10): P_{D_i} is part of the RHS, so this equation does not contain a change in the LHS. In addition, the power demand is adjusted to match the necessary gas supply. Doing so imitates a coupled network, but this is not functional for problems

where the actual amount of power-to-gas conversion is not known ahead of time.

The combined model is usable in the form described above. Its flexibility is limited by the modelling assumptions made, but it is a good place to start and it allows for some experimenting.

4

CASE STUDIES

In the previous chapter, a linear model was constructed. It remains to test and evaluate it. In the first part of this chapter, the challenges of evaluating the model's performance are discussed and a basis for comparison is established. In the second part, the structure of the network instances used in the Infrastructure Outlook is presented and we show how the elements of the combined linear model are applied to these cases.

4.1. EVALUATING THE MODEL

4.1.1. COMPARISON WITH MODELS FROM THE LITERATURE

The combined model under study consists of two components which are evaluated in distinct ways. The first is the transport load model, which is used to compute optimal flow in the pipes of the gas network (given gas entries and exits). The second is the DC power flow model, which is used to compute optimal power generation at the nodes as well as the resulting power flows. Alternatively, transport load may be minimized over the whole network.

Since the two component networks influence one another, an ideal point of comparison would be a case study in which a combined gas and power network is simulated using a more accurate model and all the necessary input data are given, as well as the resulting outputs: the power generated at each node, and the flow in each gas pipe. However, literature providing all of this is scarce. Input data can be found without too much difficulty. In particular, data for a variety of coupled networks can be found at `http://motor.ece.iit.edu/data/`. Output data, on the other hand, are more challenging to find: many papers give only partial results, such as costs, computation time, or plots showing the evolution of each quantity.

Another potential hurdle is the lack of *comparable* data. For example, in [13], all the necessary data are available, but the quadratic generation costs of the power network prevent the use of linear programming. Using only the linear component changes the problem, so it is no surprise that the solution is quite different. Other issues include a lack of degrees of freedom, as in [16]: the gas network used there had no loops and thus

only one solution for gas flow; no optimization can take place. Therefore, the solution obtained is exactly that given in the original paper, which is of limited interest.

4.1.2. EVALUATION BY APPLICATION TO A TEST NETWORK

In order to get around the lack of immediately comparable results in the literature, a different procedure is used. A test network is constructed out of two components whose full solution is available, along with a single coupling link between the two. First, the linear model is used to solve for each flow and this is compared against the known solution. Then, the flows in the combined network are compared with those in the decoupled component networks. The first step allows us to evaluate the impact of the choice of model, while the second lets us verify that the model is correctly constructed and implemented and gives an idea of the potential impact of coupling.

COMPONENTS

The chosen component networks need to be small enough to manipulate easily, and to have loops so that optimization can take place. Additionally, the generator costs in the power network need to be linear.

The chosen gas network is the first case study described in [14], which we refer to as AL9. One modification is made: since the lengths of the pipes are identical in the original network, they are each arbitrarily modified by multiples of 10^{-3} so that each length is unique and the optimization problem has a unique solution.

For the power network, the PJM 5-bus network (PJM5) presented in [26] fits the constraints. It also has the advantage of being one of the available examples of MATPOWER[24], which makes it very easy to obtain results.

COUPLING

The first combined network consists of AL9 and PJM5 coupled by a gas-fired generator. All the gas demand at node 3 of AL9 is used to provide energy for generator 1 of PJM5, as illustrated in fig. 4.1.

For the second combined network, the same two components are coupled by a power-to-gas plant. It uses the power leaving node 2 of PJM5 to provide gas at node 1 of AL9, which is the only source of gas in the network. This network is illustrated by fig. 4.2

4.2. APPLICATION TO A LIFE-SIZE NETWORK

As the last step of this work, a potential future combined network for the Netherlands is studied. This phase is the high point of the project; it gives insight into the weaknesses of the transport load model and potential future uses for the combined model.

4.2.1. THE DUTCH NETWORK

A map of the network under study is shown in fig. 4.3. It consists of a power network, a hydrogen network and a natural gas network. Three instances of the same network, representing snapshots at different times, are studied. That is, we look at one network with three different sets of energy inputs and outputs. The natural gas network is omitted; only the power and hydrogen networks are included in the study. The instances are identified by three letters indicating the energy production scenario (regional, national

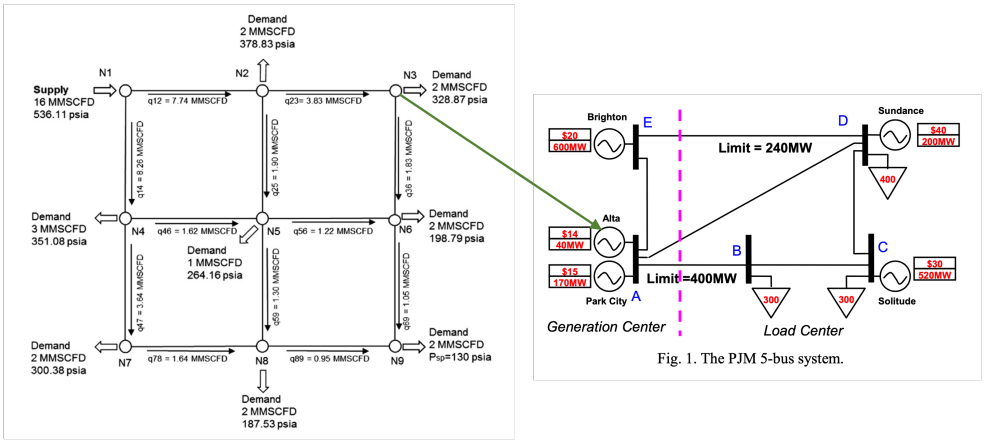

Fig. 1. The PJM 5-bus system.

4

Figure 4.1: Combined network composed of AL9 and PJM5 coupled by a gas-fired generator

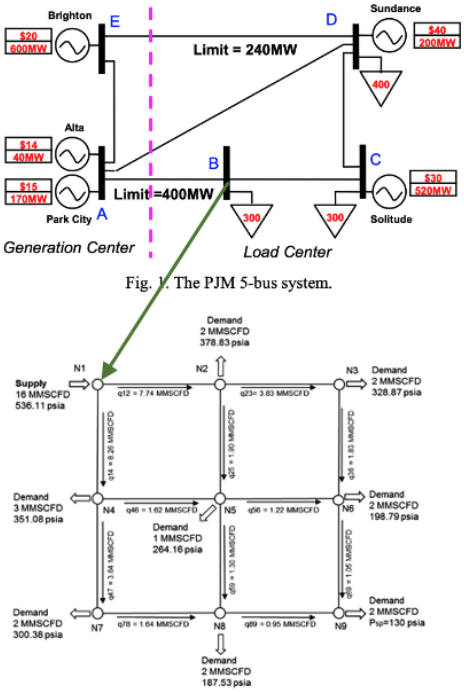

Fig. 1. The PJM 5-bus system.

Figure 4.2: Combined network composed of AL9 and PJM5 coupled by a power-to-gas plant

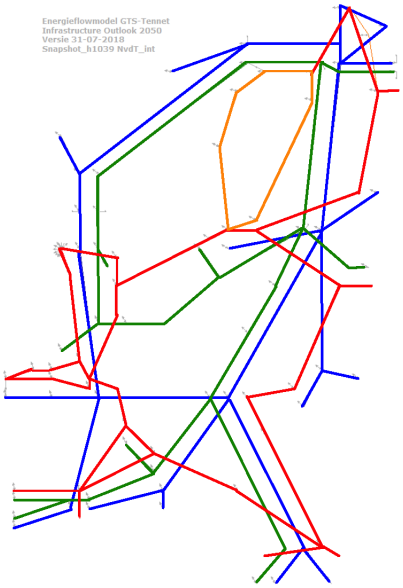

Figure 4.3: Combined network of the Netherlands (red/orange = electricity; blue = hydrogen; green = methane)

or international) and a number which is the hour (in the year) at which the snapshot is obtained. The instances under study are REG 0834 (early February, regional energy production), INT 1039 (mid-February, international scenario) and NAT 4044 (mid-June, national scenario). We refer to them only by their number in the rest of this document.

The case data include all the energy inputs and outputs, including those coming from points of coupling. In practice, this means that all that is left to do is compute the load flows in the component networks separately: transport load is used for the hydrogen and power networks, and DC power flow is computed as well and compared against optimal power transport load.

4.2.2. COMPARISON WITH THE INFRASTRUCTURE OUTLOOK MODEL

For these network instances, full solution data are available. This allows us to compare the given energy flows with the ones calculated using the combined model. For the gas components, both sets of flows are computed by minimizing transport loads, so we can verify that the model's implementation is correct by checking that the results match the given solution. For the power component, the same can be done, and additionally the flows obtained with transport load and with the DC model are compared. We expect the solution with transport load to differ significantly from the more exact solution with the DC model. The transport load model may therefore lead to incorrect conclusions about the viability of the network configuration.

The two steps of model evaluation and model application which are described in this chapter could each be the object of an entire thesis. On the one hand, evaluating the accuracy of the transport load model for gas is not an easy task, and especially not in the case of combined networks. On the other hand, the Dutch networks could be studied more thoroughly, for example by calculating energy inputs using the combined model. Combining the two is an interesting task but necessarily limits the amount of work that can be done for each.

5

RESULTS AND DISCUSSION

THis chapter presents and discusses the results of the experiments described in chapter 4. In the first section, we deal with the evaluation of the combined model using small test networks. In the second, we show the result of computing gas flows with transport load optimization, and compare optimal power transport load to DC power flow.

5.1. MODEL EVALUATION USING TEST NETWORKS

This step is divided in two: First, the components are looked at separately in order to evaluate the impact of the choice of model. Next, the components are coupled and the impact of coupling on the power network is examined.

5.1.1. IMPACT OF THE MODEL: A LOOK AT THE COMPONENTS

GAS NETWORK

The gas flows computed in [14] are compared to the optimal transport load in AL9. They are respectively shown in fig. 5.1a and fig. 5.1b. Figure 5.1c shows that there is a large difference between the two sets of flows. This can be explained by multiple factors: first, the arbitrary modification of the pipe lengths alters the solution. The longest pipes (which

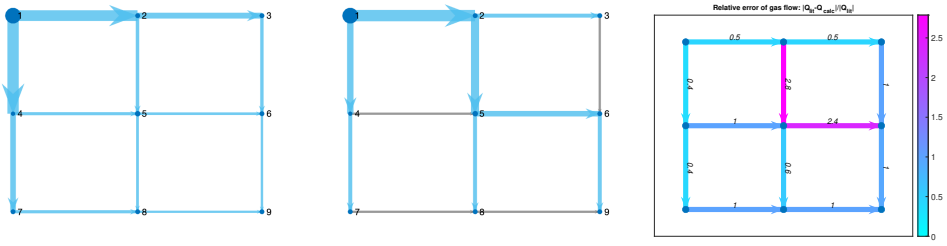

(a) Gas flows in AL9 according to [14] (b) Optimal transport load in AL9 (c) Relative error

Figure 5.1: Gas flows in decoupled AL9

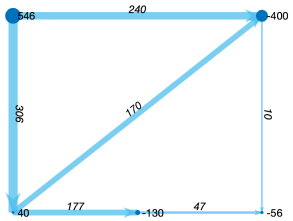

(a) Optimal DC power flow in PJM5

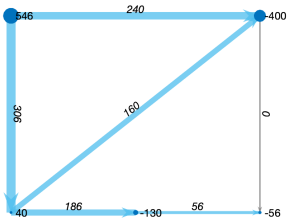

(b) Optimal power transport load in PJM5

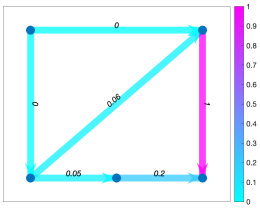

(c) Relative error

Figure 5.2: Power flows in decoupled PJM5

have the highest cost) are not used at all, and all the flow is directed through the shortest ones since there are no limits on pipe capacity in this example. In addition, the result of [14] is not necessarily an optimal flow pattern. This example shows that while transport load is potentially able to give a plausible qualitative picture of flow behaviour, it is still a rough approximation.

POWER NETWORK

For this step, DC OPF is computed first, then the resulting power generation data are used to compute optimal transport load. As a result, the net power injection at the nodes is identical in the two versions. The resulting flows patterns are similar: in most lines, the difference is very small, as can be seen in fig. 5.2c. Only in the rightmost line is there a large error value; this is because the flow is 10 MW with DC power flow and 0 MW with the TL model. The absolute difference is not so large, but the relative difference is.

One possible explanation for the similarities of the two results is that the quantities being optimized are not the same, but DC OPF does take into account the reactance of the lines. Since this quantity is proportional to the line length (see appendix A), it is hardly surprising that the result looks close to the optimal transport load. In addition, the network is small and has few degrees of freedom, which further helps the transport load approach the correct solution given by DC equations.

REMARKS

From these sample networks, we can get a general idea of what level of accuracy can be expected from these linear models. However, given the small size of the networks and the fact that a single point of comparison was used in both cases, the results cannot easily be generalized and further study would be useful.

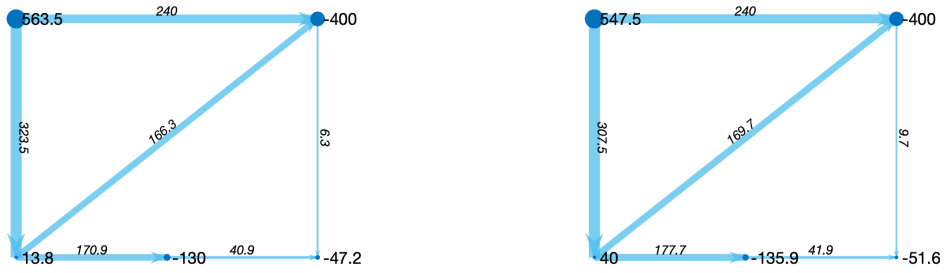

(a) Power flow in PJM5 with a GFG link ending at node 1

(b) Power flow in PJM5 with a PtG link starting at node 2

Figure 5.3: Power flows in coupled PJM5

5.1.2. IMPACT OF COUPLING

By construction, in the two coupled networks constructed out of AL9 and PJM5, the gas flow pattern remains identical to the one in the decoupled version. We thus omit to show the gas component. What changes is the power injection at one end of the coupling link, which causes some change in power generation and power flow.

The results are shown in fig. 5.3. In fig. 5.3a, we see the flows in the power component of the network represented in fig. 4.1. All the gas leaving node 3 of AL9 is used to produce power at node 1, which has the lowest generation cost. Power production is therefore limited by the availability of gas and this is visible in the figure. The second cheapest generator is at node 2 and already works at full capacity in the decoupled version, so the lacking power is produced by the third cheapest, at node 5. Figure 5.3b shows the flows for the power network in fig. 4.2. This time, all the power demand at node 2 is directed towards the production of gas at node 1 of AL9. This slightly reduces the power demand at node 2 and thus the most expensive generator, at node 3, produces less power.

As expected, both networks look much the same as the decoupled PJM5. This result cannot easily be generalized, however, since the construction of these particular coupled networks deeply influences the results. These examples are useful as an exercise and for checking that the model is correctly implemented, but their use as a reference on the impact of coupling is limited.

5.2. THE DUTCH NETWORKS

In this section, the study of one network configuration used in the Infrastructure Outlook is presented. Three sets of energy entries and exits (instances), corresponding to different times of the year and energy production scenarios, are studied. Transport load is used to compute gas flow in the hydrogen and natural gas components of the network. For the power network, DC PF is computed using the PTDF matrix of the network and the power injection data. Power flows are also computed using transport load and the two sets of results are compared.

Communication between components is not modeled explicitly. Instead, injection data for each component includes energy coming from coupling links: electrolysis, metha-

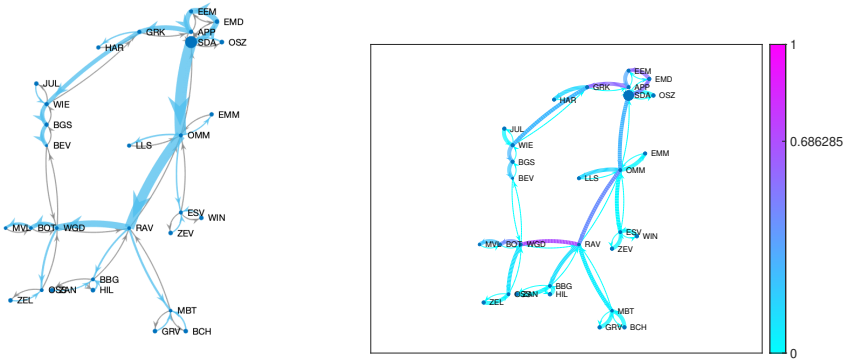

(a) Optimal transport load of hydrogen

(b) Flow of hydrogen compared to pipe capacity

Figure 5.4: Hydrogen flows in instance 1039

5

nation and gas-fired generators. This means that the component networks can be studied separately.

We look in detail at instance 1039 and briefly compare it to the other two. The full set of plots is shown in appendix E.

5.2.1. HYDROGEN COMPONENT

For this part, since the model used is the same as in the Infrastructure Outlook, we are looking to match the results. This is indeed the case: calculating the error in pipe k as

$$e_k = \frac{Q_k^{sol} - Q_k^{calc}}{Q_k^{sol}},$$

the largest e_k observed is about 0.5% over all three instances. Another common point between the instances is that the capacity limits of the lines are not reached (i.e., line capacities are not binding constraints). An interesting result of this is that the flows form a minimal spanning tree of the network. Indeed, gas is transported from node i to node j via the shortest path (in length) unless a pipe on that path is saturated. In that case, the excess is routed through another path, but as that is not happening, only shortest paths are used and no loops appear.

The results of the calculations for instance 1039 are shown in fig. 5.4. On one hand, fig. 5.4a shows the general behaviour of the gas flow. The largest quantities flow in two main pipes, one of which, unsurprisingly, leaves from node SDA, which has the largest net gas injection (represented by node size). These two pipes carry gas that is provided to the entire southern half of the network. On the other hand, in fig. 5.4b, we see how saturated each of these pipes are. The ones carrying the most gas are not the most saturated, though the busiest one (RAV-WGD, at 68% of its capacity) also carries a relatively large amount. For a gas network, this is an acceptable state.

Comparable levels of saturation can be observed in instance 4044. On the other hand, instance 0834 deals with smaller quantities of hydrogen and is much further from overload (its busiest pipe is used only at 13% of its capacity).

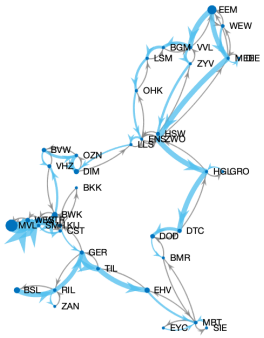

(a) Optimal transport load of power

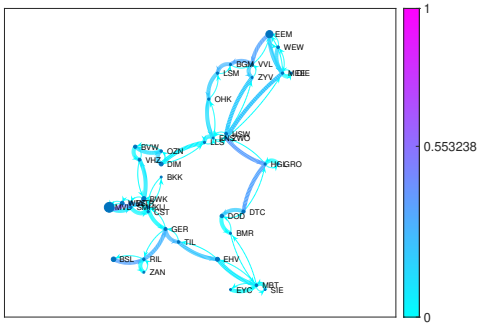

(b) Flow of power compared to line capacity

Figure 5.5: Power transport load in instance 1039

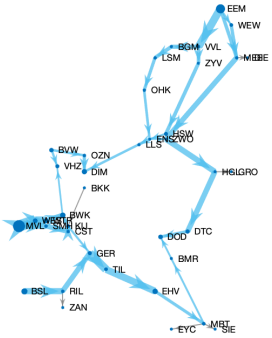

(a) DC power flows

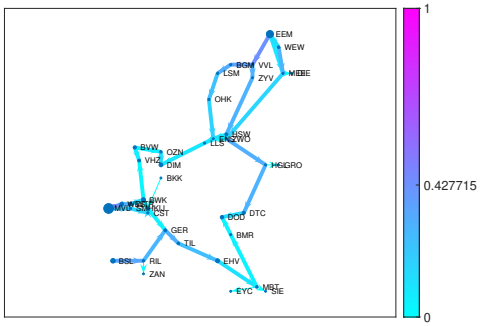

(b) DC power flows compared to line capacity

Figure 5.6: DC power flows in instance 1039

5.2.2. POWER COMPONENT

We first look at power flows as calculated with transport load optimization. The results of the Infrastructure Outlook were matched in this case as well. The results are visible in fig. 5.5, with fig. 5.5b showing that the busiest line operates at 55 % of its capacity. While this is technically feasible, $N-1$ security constraints mean that this is not an acceptable state of the network.

Next, we look at DC power flow, which is represented in fig. 5.6. To check that it is correctly calculated, we look at the flow in radial lines: indeed, six of the radial nodes (BKK, DIE, EYC, GRO, SIE, ZAN) have zero power injection, so the line linking them to the rest of the network should contain zero flow, or a very small value due to round-off error. At the last radial node (BSL, at the bottom left), the net power injection is positive, so power should be flowing away from that node. This is the case for all three instances, which is a good indication that the flows are correctly computed.

Though the two flow patterns (TL and DC) display qualitatively comparable behaviours,

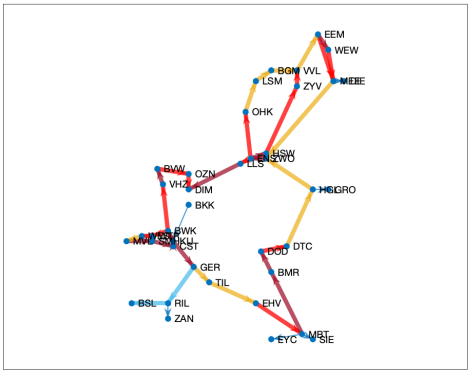

Figure 5.7: Relative difference between DC and TL power flow, $|P_{dc} - P_{tl}|/|P_{dc}|$.
Error e: thin blue lines $e = 0$, light blue $0 < e \leq 0.1$, yellow $0.1 < e \leq 0.25$, red $0.25 < e \leq 1$, dark red $e \geq 1$

5

the difference shown in fig. 5.7 makes it clear that the TL model is incorrect. The error is under 10% only in lines with no degrees of freedom, i.e. radial lines. In the rest of the network, there is a major difference between TL and DC flows. In particular, the maximum line saturation over the whole network is only 43% in the DC model, which makes the state of the network acceptable and contradicts the answer given by the TL model.

As for the other two instances, they also display large differences between the two models (see appendix E). However, in both cases, the network is in an unacceptable state regardless of the model used.

Such large differences are somewhat expected, since it was known ahead of time that transport load optimization is not a correct way to model power flows. This experiment shows how unreliable it can be.

5.2.3. NATURAL GAS COMPONENT

As mentioned in the previous chapter, the natural gas component is not included in this analysis. Indeed, the goal of this part is to match previously obtained results for the gas networks, since no modification is made to the transport load model. Combined with time limitations, this meant that adding the natural gas flows to this chapter had limited interest.

5.2.4. GENERAL REMARKS

In all three cases, the time necessary to carry out the computations is very short. A script which runs the transport load optimization function on both the power and hydrogen network and also computes DC power flows takes about 0.2 seconds to run in Matlab once all the necessary data are in the workspace. This is fast enough that the model can be used to quickly compute the 8760 hourly snapshots over a year, even once the natural gas network is added in. This allows to test many different network configurations in reasonably short times.

It is clear from both sets of experiments presented in this chapter that the choice of model has a major impact on the results. We are now able to quantify this for the transport load and DC model in power networks. On the other hand, we have very limited data for gas networks due to the difficulty of comparing models purely on the basis of existing literature. An ideal way to compare models for gas would have been to implement and solve the full nonlinear equations. That is, however, outside the scope of this thesis and will need to be done in a future project.

6

CONCLUSIONS AND FUTURE WORK

The stated goal of this thesis was to construct, evaluate and apply a combined linear model improving on the one used in the Infrastructure Outlook (IO) report of Gasunie and TenneT. The literature review showed that while a sizeable body of literature exists on models of combined energy networks, virtually all of it seeks accuracy rather than scalability. Conversely, the IO results are based on transport load (TL) optimization for all the energy carriers, which is a very simplified and computationally inexpensive model.

In chapter 3, the construction step is detailed. A combined model was constructed out of TL for gas networks and DC equations for the power network. Communication between the two was modelled via power-to-gas and gas-to-power links. Bidirectional coupling was not directly modelled, as it would require extra optimization steps to determine when it would be advantageous to use both couplings simultaneously. In addition, since this form of the model relies on pre-calculated (optimal) production of energy, the combined model does as well (at least for the gas network). Thus, an auxiliary model, or an expanded version of the current one, is still needed for applications.

The evaluation step constitutes the first part of chapter 4 and of chapter 5. The literature of coupled energy networks lacks case studies with which direct comparison is possible, so a different process was used. First, the impact of the choice of model was studied: transport load was compared to the standard gas flow model in a small gas network, and to DC power flow in a small power network. Next, the flows obtained for the test power network with the combined model were compared to those calculated for the decoupled network as a way to examine the impact of coupling. This was not done for the gas network, since the construction of the model meant that coupling did not affect it. By affecting the distribution of power demand and power generation, coupling affects power flows accordingly, showing that the model is functional.

Finally, the different elements of the combined model were used to compute energy flows in the components of a realistic Dutch energy network. The results for the hydrogen network matched the provided solution data, demonstrating that this part of the model was correctly implemented. Additionally, a major improvement in accuracy was

achieved in the computation of power flows thanks to the use of the DC model.

The main conclusions of this thesis are the following:

1. **The transport load optimization model is incorrect for power network simulation and should not be used**.

   DC power flow produces good results and is widely accepted; it is therefore a better choice of linear model for power networks.

2. **TL optimization for gas networks gives a rough first indication of optimal flows but its accuracy must be investigated further.**

   So far, this investigation has been done only in a small example network. A more thorough evaluation would require obtaining the full input and output data of at least one larger gas network, which is difficult to find in the literature; or computing gas flow patterns using the standard nonlinear model, which was outside the scope of this project.

3. **Coupling a DC OPF power network and a TL optimized gas network has not been done before for sizable networks, but it may yield useful results.**

   A combined model was constructed and shown to be functional for small test networks. In addition, the calculations carried out based on Dutch network data took very little time to compute. Further work will be necessary to generalize the combined model for use with the Dutch network and quantify its accuracy. This thesis shows that the combined model may be suitable at highly aggregated levels, for example for the Dutch energy system of 2050.

BIBLIOGRAPHY

[1] M. Götz, J. Lefebvre, F. Mörs, *et al.*, "Renewable Power-to-Gas: A technological and economic review," en, *Renewable Energy*, vol. 85, pp. 1371–1390, Jan. 2016, ISSN: 0960-1481. DOI: 10.1016/j.renene.2015.07.066. [Online]. Available: https://www.sciencedirect.com/science/article/pii/S0960148115301610 (visited on 04/09/2021).

[2] M. Nazari-Heris, S. Asadi, and B. Mohammadi-Ivatloo, Eds., *Planning and Operation of Multi-Carrier Energy Networks*, en, ser. Power Systems. Springer International Publishing, 2021, ISBN: 978-3-030-60085-3. DOI: 10.1007/978-3-030-60086-0. [Online]. Available: https://www.springer.com/gp/book/9783030600853 (visited on 04/16/2021).

[3] S. An, Q. Li, and T. W. Gedra, "Natural gas and electricity optimal power flow," in *2003 IEEE PES Transmission and Distribution Conference and Exposition (IEEE Cat. No.03CH37495)*, vol. 1, Sep. 2003, 138–143 Vol.1. DOI: 10.1109/TDC.2003.1335171.

[4] M. Lehner, R. Tichler, H. Steinmüller, and M. Koppe, *Power-to-Gas: Technology and Business Models*, en, ser. SpringerBriefs in Energy. Springer International Publishing, 2014, ISBN: 978-3-319-03994-7. DOI: 10.1007/978-3-319-03995-4. [Online]. Available: https://www.springer.com/gp/book/9783319039947 (visited on 04/02/2021).

[5] "Infrastructure Outlook 2050," en, Gasunie and TenneT, Tech. Rep., 2020. [Online]. Available: https://www.gasunie.nl/en/expertise/system-integration/infrastructure-outlook-2050.

[6] M. Shahidehpour, Yong Fu, and T. Wiedman, "Impact of Natural Gas Infrastructure on Electric Power Systems," *Proceedings of the IEEE*, vol. 93, no. 5, pp. 1042–1056, May 2005, Conference Name: Proceedings of the IEEE, ISSN: 1558-2256. DOI: 10.1109/JPROC.2005.847253.

[7] M. Geidl and G. Andersson, "Optimal Power Flow of Multiple Energy Carriers," *IEEE Transactions on Power Systems*, vol. 22, no. 1, pp. 145–155, Feb. 2007, Conference Name: IEEE Transactions on Power Systems, ISSN: 1558-0679. DOI: 10.1109/TPWRS.2006.888988.

[8] A. Martinez-Mares and C. R. Fuerte-Esquivel, "A Unified Gas and Power Flow Analysis in Natural Gas and Electricity Coupled Networks," *IEEE Transactions on Power Systems*, vol. 27, no. 4, pp. 2156–2166, Nov. 2012, Conference Name: IEEE Transactions on Power Systems, ISSN: 1558-0679. DOI: 10.1109/TPWRS.2012.2191984.

[9] G. Li, R. Zhang, T. Jiang, H. Chen, L. Bai, and X. Li, "Security-constrained bi-level economic dispatch model for integrated natural gas and electricity systems considering wind power and power-to-gas process," en, *Applied Energy*, vol. 194, pp. 696–704, May 2017, ISSN: 0306-2619. DOI: 10.1016/j.apenergy.2016.07.077. [Online]. Available: https://www.sciencedirect.com/science/article/pii/S0306261916310194 (visited on 04/16/2021).

[10] S. Chatzivasileiadis, *Optimization in Modern Power Systems. Lecture notes*. Nov. 2018. [Online]. Available: www.chatziva.com/teaching/2017/31765/Lectures/31765_Lecture10.pdf.

[11] T. v. d. Hoeven, *Math in gas and the art of linearization*, en. Groningen: Energy Delta Institute, 2004, OCLC: 249380545, ISBN: 978-90-367-1990-2.

[12] S. Menon, *Gas Pipeline Hydraulics*, en. CRC Press, May 2005, ISBN: 978-0-429-12410-5. DOI: 10.1201/9781420038224. [Online]. Available: https://www.taylorfrancis.com/https://www.taylorfrancis.com/books/mono/10.1201/9781420038224/gas-pipeline-hydraulics-shashi-menon (visited on 04/01/2021).

[13] J. Beyza, J. A. Dominguez-Navarro, and J. M. Yusta, "Linear-analog transformation approach for coupled gas and power flow analysis," en, *Electric Power Systems Research*, vol. 168, pp. 239–249, Mar. 2019, ISSN: 0378-7796. DOI: 10.1016/j.epsr.2018.11.012. [Online]. Available: https://www.sciencedirect.com/science/article/pii/S0378779618303730 (visited on 03/29/2021).

[14] L. F. Ayala H. and C. Y. Leong, "A robust linear-pressure analog for the analysis of natural gas transportation networks," en, *Journal of Natural Gas Science and Engineering*, vol. 14, pp. 174–184, Sep. 2013, ISSN: 1875-5100. DOI: 10.1016/j.jngse.2013.06.008. [Online]. Available: https://www.sciencedirect.com/science/article/pii/S1875510013000528 (visited on 05/17/2021).

[15] Y. Tan, X. Wang, and Y. Zheng, "A new modeling and solution method for optimal energy flow in electricity-gas integrated energy system," en, *International Journal of Energy Research*, vol. 43, no. 9, pp. 4322–4343, 2019, ISSN: 1099-114X. DOI: 10.1002/er.4558. [Online]. Available: https://onlinelibrary.wiley.com/doi/abs/10.1002/er.4558 (visited on 07/05/2021).

[16] C. Unsihuay, J. W. M. Lima, and A. C. Z. d. Souza, "Modeling the Integrated Natural Gas and Electricity Optimal Power Flow," in *2007 IEEE Power Engineering Society General Meeting*, ISSN: 1932-5517, Jun. 2007, pp. 1–7. DOI: 10.1109/PES.2007.386124.

[17] C. He, X. Zhang, T. Liu, L. Wu, and M. Shahidehpour, "Coordination of Interdependent Electricity Grid and Natural Gas Network—a Review," en, *Current Sustainable/Renewable Energy Reports*, vol. 5, no. 1, pp. 23–36, Mar. 2018, ISSN: 2196-3010. DOI: 10.1007/s40518-018-0093-9. [Online]. Available: https://doi.org/10.1007/s40518-018-0093-9 (visited on 03/19/2021).

[18] "Verkenning waterstofinfrastructuur," nl, DNV GL, Tech. Rep. OGNL.151886, Rev. 2, Nov. 2017, p. 24. [Online]. Available: https://www.topsectorenergie.nl/sites/default/files/uploads/TKI%20Gas/publicaties/DNVGL%20rapport%20verkenning%20waterstofinfrastructuur_rev2.pdf.

[19] Q. Zeng, J. Fang, J. Li, and Z. Chen, "Steady-state analysis of the integrated natural gas and electric power system with bi-directional energy conversion," en, *Applied Energy*, vol. 184, pp. 1483–1492, Dec. 2016, ISSN: 0306-2619. DOI: 10.1016/j.apenergy.2016.05.060. [Online]. Available: https://www.sciencedirect.com/science/article/pii/S0306261916306572 (visited on 05/04/2021).

[20] M. Qadrdan, M. Abeysekera, M. Chaudry, J. Wu, and N. Jenkins, "Role of power-to-gas in an integrated gas and electricity system in Great Britain," en, *International Journal of Hydrogen Energy*, vol. 40, no. 17, pp. 5763–5775, May 2015, ISSN: 0360-3199. DOI: 10.1016/j.ijhydene.2015.03.004. [Online]. Available: https://www.sciencedirect.com/science/article/pii/S0360319915005418 (visited on 05/04/2021).

[21] F. Tabkhi, "Optimization of gas transport networks," English, Ph.D. dissertation, Institut National Polytechnique de Toulouse, Toulouse, 2007. [Online]. Available: https://oatao.univ-toulouse.fr/7665/1/tabkhi.pdf.

[22] Y.-Q. Bao, M. Wu, X. Zhou, and X. Tang, "Piecewise Linear Approximation of Gas Flow Function for the Optimization of Integrated Electricity and Natural Gas System," *IEEE Access*, vol. 7, pp. 91 819–91 826, 2019, Conference Name: IEEE Access, ISSN: 2169-3536. DOI: 10.1109/ACCESS.2019.2927103.

[23] A. S. Markensteijn, J. E. Romate, and C. Vuik, "A graph-based model framework for steady-state load flow problems of general multi-carrier energy systems," en, *Applied Energy*, vol. 280, p. 115 286, Dec. 2020, ISSN: 0306-2619. DOI: 10.1016/j.apenergy.2020.115286. [Online]. Available: https://www.sciencedirect.com/science/article/pii/S0306261920307984 (visited on 04/02/2021).

[24] R. D. Zimmerman, C. E. Murillo-Sánchez, and R. J. Thomas, "MATPOWER: Steady-State Operations, Planning, and Analysis Tools for Power Systems Research and Education," *IEEE Transactions on Power Systems*, vol. 26, no. 1, pp. 12–19, Feb. 2011, Conference Name: IEEE Transactions on Power Systems, ISSN: 1558-0679. DOI: 10.1109/TPWRS.2010.2051168.

[25] M. Schmidt, D. Aßmann, R. Burlacu, *et al.*, "GasLib—A Library of Gas Network Instances," *Data*, vol. 2, p. 40, Dec. 2017. DOI: 10.3390/data2040040.

[26] F. Li and R. Bo, "Small test systems for power system economic studies," in *IEEE PES General Meeting*, ISSN: 1944-9925, Jul. 2010, pp. 1–4. DOI: 10.1109/PES.2010.5589973.

[27] D. Luenberger and Y. Ye, *Linear and Nonlinear Programming*. Jan. 1984, vol. 67, Journal Abbreviation: American Journal of Agricultural Economics Publication Title: American Journal of Agricultural Economics. DOI: 10.2307/1240727.

[28] L. Vandenberghe, *Piecewise linear programming. Lecture notes*, 2013. [Online]. Available: http://www.seas.ucla.edu/~vandenbe/ee236a/lectures/pwl.pdf.

A

COMPUTING POWER FLOWS USING THE PTDF MATRIX

Power flows are computed as follows [10], [24]. The basic data necessary are the line susceptances, which are listed in vector $\mathbf{b} = (b_1, \ldots, b_N)$, and the network's branch-node incidence matrix M, which is given by

$$M_{ij} = \begin{cases} +1, \text{ if branch } j \text{ enters node } i, \\ -1, \text{ if branch } j \text{ leaves node } i, \\ 0, \text{ if branch } j \text{ is not connected to node } i. \end{cases}$$

The susceptance of a line is often given per km length, and can thus be calculated from its length L. The 380 kV lines which make up the high-tension network of the Netherlands have a reactance per length of 0.25 Ω/km, i.e. $x = 0.25L$. The susceptance is then

$$b = \frac{1}{x} = \frac{4}{L}.$$

From this, we form first the line susceptance matrix,

$$B_{\text{line}} = \text{diag}(\mathbf{b}) \cdot M^{\top} \tag{A.1}$$

then the bus susceptance matrix,

$$B_{\text{bus}} = M \cdot B_{\text{line}}. \tag{A.2}$$

The entries of the bus susceptance matrix are as follows:

- Diagonal elements B_{ii}: sum of line susceptances of all lines connected to bus i, $B_{ii} = \sum_k b_{ik}$
- Off-diagonal elements: $B_{ij} = b_{ij}$ if there is a line between nodes i and j, $B_{ij} = 0$ otherwise.

The matrix is singular, and thus not invertible. A pseudo-inverse $\tilde{B}_{\text{bus}}^{-1}$ is computed using the following procedure:

1. Remove the row and column of B_{bus} corresponding to the index of the slack bus
2. Invert the resulting matrix
3. Insert a row and a column of zeros at the indices corresponding to the slack bus.

Finally, the PTDF matrix is given by:

$$\text{PTDF} = B_{\text{line}} \tilde{B}_{\text{bus}}^{-1} \tag{A.3}$$

It relates the line flows to the power injection at nodes as follows:

$$P_{\text{line}} = \text{PTDF} \cdot (\mathbf{P}_G - \mathbf{P}_D). \tag{A.4}$$

Alternatively, for known power injection (which is the case with the Dutch network data, but not when computing DC OPF from scratch), line flows can be computed by solving for the bus voltage angles. Indeed, the net power injection at nodes $\mathbf{P}_{\text{bus}}$ is related to the voltage angles δ by

$$\mathbf{P}_{\text{bus}} = B_{\text{bus}} \delta \tag{A.5}$$

and the flow in lines $\mathbf{P}_{\text{line}}$ is related to δ by

$$\mathbf{P}_{\text{line}} = B_{\text{line}} \delta. \tag{A.6}$$

Line flows are then obtained by solving eq. (A.5) for δ, then applying eq. (A.6).

B

PRINCIPLES OF LINEAR OPTIMIZATION

Optimization, or mathematical programming, is the process of finding the *best possible value* of a variable, based on some criterion and usually under a set of constraints. For instance, when minimizing a function $f(\mathbf{x})(\mathbf{x} \in \mathbb{R}^n)$, the optimal value $\mathbf{x}^*$ of $\mathbf{x}$ is the one that yields the smallest value of f. The function f is called *cost* or *objective* function. Constraints may be equations of the form $g(\mathbf{x}) = a$, inequalities of the form $h(\mathbf{x}) \leq b$, or bounds on the elements of $\mathbf{x}$.

Throughout this report, we use linear optimization. That is, the function to be minimized and all its constraints are linear. Such a problem can always be (re-)written in the standard form [27]:

$$\begin{array}{ll} \text{Find a vector} & \mathbf{x} \\ \text{that maximizes} & \mathbf{c}^T\mathbf{x} \\ \text{subject to} & A\mathbf{x} = \mathbf{b} \\ \text{and} & \mathbf{x} \geq \mathbf{0} \end{array} \tag{B.1}$$

It is quite easy to find a particular solution that satisfies the constraints. First, consider the system of inequalities

$$A\mathbf{x} = \mathbf{b}. \tag{B.2}$$

where $\mathbf{x}$ is an n-vector, $\mathbf{b}$ an m-vector, and A is an $m \times n$ matrix. Suppose that from the n columns of A we select a set of m linearly independent columns (such a set exists if the rank of A is m). For simplicity, we assume that the first m columns of A constitute this set and we denote by B the $m \times m$ matrix formed by these columns. Then, the matrix B is nonsingular and the equation

$$B\mathbf{x}_B = \mathbf{b}$$

has a unique solution $\mathbf{x}_B$, and $\mathbf{x} = (\mathbf{x}_B, \mathbf{0})$ is a solution to $A\mathbf{x} = \mathbf{b}$. This is called a *basic solution* to *eq.* (B.2) with respect to the basis B. The existence of a basic solution relies on the *full rank assumption*: The $m \times n$ matrix A has $m < n$, and the m rows of A are linearly independent.

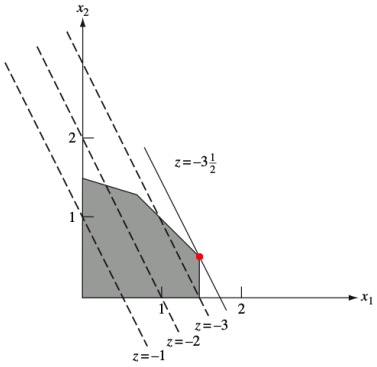

Figure B.1: Illustration of an extreme point solution

We can now add in the other constraint of eq. (B.1). Consider the system of constraints

$$\begin{aligned} A\mathbf{x} &= \mathbf{b} \\ \mathbf{x} &\geq \mathbf{0} \end{aligned} \tag{B.3}$$

A vector $\mathbf{x}$ satisfying eq. (B.3) is said to be *feasible* for these constraints. If it is in addition a basic solution of eq. (B.2), it is said to be a *basic feasible solution*. The set of feasible vectors of eq. (B.3) is called the *feasible set* of the problem.

Relation to convexity A set C is said to be *convex* if for every $\mathbf{x}_1, \mathbf{x}_2 \in C$ and every real number α with $0 < \alpha < 1$, the point $\alpha\mathbf{x}_1 + (1-\alpha)\mathbf{x}_2 \in C$. This definition can be interpreted geometrically as stating that a set is convex if, given two points in the set, every point on the line segment joining these two points is also a member of the set. The feasible set of a problem of the form eq. (B.3) is convex.

A point $\mathbf{x}$ in a convex set C is said to be an *extreme point* of C if there are no two distinct points $\mathbf{x}_1, \mathbf{x}_2 \in C$ such that $\mathbf{x} = \alpha\mathbf{x}_1 + (1-\alpha)\mathbf{x}_2$. Geometrically, it is a point that does not lie strictly within a line segment connecting two other points of the set. The extreme points of a triangle, for example, are its three vertices.

Theorem (Equivalence of extreme points and basic solutions) *Let A be an $m \times n$ matrix and $\mathbf{b}$ an m-vector. Let K be the convex set consisting of all n-vectors $\mathbf{x}$ satisfying*

$$\begin{aligned} A\mathbf{x} &= \mathbf{b} \\ \mathbf{x} &\geq \mathbf{0} \end{aligned}$$

A vector $\mathbf{x}$ is an extreme point of K if and only if $\mathbf{x}$ is a basic feasible solution of the above.

This is illustrated in fig. B.1.

C

FROM PIECEWISE LINEAR TO LINEAR PROGRAMMING

C.1. PRINCIPLES

The following discussion is adapted from [28].

For the transport load minimization problem, we are looking to minimize a convex piecewise linear function with linear constraints. Such a function $f : \mathbb{R}^n \to \mathbb{R}$ can be expressed as

$$f(x) = \max_i (a_i^\top x + b_i) \qquad i = 1, ..., m \tag{C.1}$$

with $a, x, \in \mathbb{R}$ and $b \in \mathbb{R}$. f is parameterized by m n-vectors a_i and m scalars b_i.

An example is shown in fig. C.1.

The problem of minimizing such a function, $\min f(x)$, can be written as a linear program:

$$\begin{aligned} &\min t \\ &\text{subject to } a_i^\top x + b_i \le t, \quad i = 1, \ldots, m \end{aligned} \tag{C.2}$$

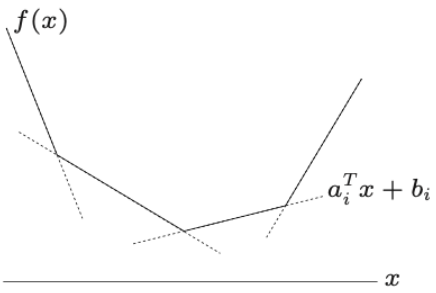

Figure C.1: Convex piecewise linear function

To see this, note that for fixed x, the optimal t is $t = f(x)$. In matrix notation, this becomes: minimize $\tilde{c}^\top \tilde{x}$ subject to $\tilde{A}\tilde{x} \leq \tilde{b}$, with

$$\tilde{x} = \begin{bmatrix} x \\ t \end{bmatrix}, \quad \tilde{c} = \begin{bmatrix} \mathbf{0} \\ 1 \end{bmatrix}, \quad \tilde{A} = \begin{bmatrix} a_1^T & -1 \\ \vdots & \vdots \\ a_m^T & -1 \end{bmatrix}, \quad \tilde{b} = \begin{bmatrix} -b_1 \\ \vdots \\ -b_m \end{bmatrix} \tag{C.3}$$

Note that other linear constraints can be added to this. We will detail them for the transport load problem.

Minimizing a sum of piecewise linear functions The sum of two piecewise linear functions of the form eq. (C.1), $f(x)$ and $g(x)$, is also piecewise linear. If f is parameterized by m vectors and g is parameterized by p vectors, their sum is the maximum of mp affine functions,

$$f(x) + g(x) = \max_{\substack{i=1,\dots,m \\ j=1,\dots,p}} \left(\left(a_i + c_j\right)^T x + \left(b_i + d_j\right) \right) \tag{C.4}$$

The equivalent linear program of $\min f(x) + g(x)$ has $m + p$ inequalities. It is given by

$$\begin{aligned} &\min t_1 + t_2 \\ \text{subject to } &a_i^\top x + b_i \leq t_1, \quad i = 1, \dots, m \\ &c_i^\top x + d_i \leq t_1, \quad i = 1, \dots, p \end{aligned} \tag{C.5}$$

Note that for fixed x, the optimal values of t_1 and t_2 are $t_1 = f(x)$ and $t_2 = g(x)$.

In matrix notation, the problem becomes: minimize $\tilde{c}^\top \tilde{x}$ subject to $\tilde{A}\tilde{x} \leq \tilde{b}$, with

$$\tilde{x} = \begin{bmatrix} x \\ t_1 \\ t_2 \end{bmatrix}, \quad \tilde{c} = \begin{bmatrix} \mathbf{0} \\ 1 \\ 1 \end{bmatrix}, \quad \tilde{A} = \begin{bmatrix} a_1^T & -1 & 0 \\ \vdots & \vdots & \vdots \\ a_m^T & -1 & 0 \\ c_1^T & 0 & -1 \\ \vdots & \vdots & \vdots \\ c_p^T & 0 & -1 \end{bmatrix}, \quad \tilde{b} = \begin{bmatrix} -b_1 \\ \vdots \\ -b_m \\ -d_1 \\ \vdots \\ -d_p \end{bmatrix} \tag{C.6}$$

C.2. APPLICATION TO TRANSPORT LOAD MINIMIZATION

In the case of the transport load function (eq. (3.6)), the optimization variable $\mathbf{Q} \in \mathbb{R}^N$ is the list of loads in each pipe. For pipe k, the transport load is

$$T_k(\mathbf{Q}) = \max_i \mathbf{L}_{i,k}^\top \mathbf{Q}$$

where all the elements of vector $\mathbf{L}_{i,k}$ are zero, except the k-th one, which is as described by eq. (3.7). This means there are 4 possible values for each L_k. The cost function is then

$$T(\mathbf{Q}) = \sum_{k=1}^{N} T_k(\mathbf{Q})$$

which is parameterized by $4N$ vectors $\mathbf{L}_{i,k}$. Generalizing eq. (C.6) to a sum of N piecewise linear functions, we obtain the following linear problem: minimize $\tilde{c}^\top \tilde{Q}$ subject to $\tilde{A}\tilde{x} \leq \tilde{b}$, with

$$\tilde{Q} = \begin{bmatrix} \mathbf{Q} \\ t_1 \\ \vdots \\ t_2 \end{bmatrix}, \quad \tilde{c} = \begin{bmatrix} \mathbf{0} \\ \mathbf{1} \end{bmatrix}, \quad \tilde{A} = \begin{bmatrix} L_{1,1} & 0 & \dots & 0 & -1 & 0 & \dots & 0 \\ \vdots & & \ddots & & \vdots & & \ddots & \\ L_{1,4} & 0 & \dots & 0 & -1 & 0 & \dots & 0 \\ 0 & L_{2,1} & \dots & 0 & 0 & -1 & \dots & 0 \\ & \vdots & & & & \vdots & & \\ 0 & L_{2,4} & \dots & 0 & 0 & -1 & \dots & 0 \\ & \ddots & & & & \ddots & & \\ 0 & \dots & 0 & L_{N,1} & 0 & \dots & 0 & -1 \\ 0 & \dots & 0 & \vdots & & \ddots & & \vdots \\ 0 & \dots & 0 & L_{N,4} & 0 & \dots & 0 & -1 \end{bmatrix}, \quad \tilde{b} = [\mathbf{0}_{4N}] \tag{C.7}$$

where $\mathbf{0}$ and $\mathbf{1}$ are the N-vectors of zeros and of ones, respectively. ($\mathbf{0}_{4N}$ is the $4N$-vector of zeros.)

It remains to add the missing equality constraints, which enforce mass conservation. This set of constraints is originally given by $M\mathbf{Q} = \mathbf{w}$. Expanding both sides to include the auxiliary variables t_k, the equality constraint in matrix form becomes

$$\tilde{A}_{\text{eq}}\tilde{Q} = \tilde{b}_{\text{eq}},$$

where

$$\tilde{A}_{\text{eq}} = \begin{bmatrix} M & \mathbf{0} \end{bmatrix} \quad \text{and} \quad \tilde{b}_{\text{eq}} = \begin{bmatrix} \mathbf{w} \\ \mathbf{0} \end{bmatrix} \tag{C.8}$$

The complete linear optimization problem is then:

$$\begin{array}{ll} \min & \tilde{c}^\top \tilde{Q} \\ \text{subject to} & \tilde{A}\tilde{x} \leq \tilde{b} \\ \text{and} & \tilde{A}_{\text{eq}}\tilde{x} = \tilde{b}_{\text{eq}} \end{array} \tag{C.9}$$

Bounds on the elements of $\mathbf{Q}$ are not necessary, since values above the lines capacities are penalized by the piecewise definition of $T(Q)$.

D

INPUT AND OUTPUT DATA OF ONE CASE STUDY

In this appendix, we give all the data necessary to reproduce the results of instance 1039, for which the plots are visible in chapter 5. As the capacity of lines is not public information, we do not give it here. However, for transport load optimization, line capacities are not binding constraints for the hydrogen or the power network. For the same reason, only the absolute flow is given, and not the line saturation data.

Table D.1: Nodes of the power component with entries and exits of INT 1039

Point	Index	Entries	Exits
E-BGM	1	31,5	120,6
E-BKK	2	0	0
E-BMR	3	312,9	330
E-BSL	4	1688,6	539,6
E-BVW	5	1289	721,1
E-BWK	6	18,2	950,6
E-CST	7	122,3	267,2
E-DIE	8	0	0
E-DIM	9	511,9	1318,8
E-DOD	10	697	1325,1
E-DTC	11	212,7	721,3
E-EEM	12	2536	266,3
E-EHV	13	132	1007,7
E-ENS	14	40,6	52,1
E-EYC	15	0	0
E-GER	16	1355,5	913,5
E-GRO	17	0	0
E-HGL	18	519,6	581,5
E-HSW	19	85	460,6
E-KIJ	20	0,2	327,1
E-LLS	21	263	360,4
E-LSM	22	116	269,9
E-MBT	23	539,4	812,3
E-MEE	24	186,8	300,6
E-MVL	25	4959,9	1552,4
E-OHK	26	20,3	148,2
E-OZN	27	1241,2	1048,2
E-RIL	28	187,4	399,8
E-SIE	29	0	0
E-SMH	30	0,2	196,2
E-TIL	31	34,4	315,6
E-VHZ	32	3,4	398,6
E-VVL	33	27,4	248,9
E-WES	34	0,1	694,4
E-WEW	35	438,3	167,7
E-WTR	36	56,2	810,3
E-ZAN	37	0	0
E-ZWO	38	0	0
E-ZYV	39	234,2	234,6

From	To	From index	To index	Length (km)	Flow (TL)	Flow (DC)
E-BGM	E-VVL	1	33	32,5	-613,1124878	-701.24
E-BKK	E-KIJ	2	20	57,5	0	0
E-BMR	E-DOD	3	10	42	-17,16266036	160.15
E-BVW	E-OZN	5	27	16,1	480,537529	303.35
E-BWK	E-WTR	6	36	21,9	-1618,264465	-876.72
E-CST	E-KIJ	7	20	14,8	0	741.58
E-DOD	E-DTC	10	11	44,6	-645,2857208	-467.85
E-DTC	E-HGL	11	18	58,7	-1153,905792	-976.55
E-EEM	E-MEE	12	24	37,6	1059,046402	539.5
E-EEM	E-WEW	12	35	24,3	0	230.53
E-EHV	E-MBT	13	23	48,8	272,8596878	450.05
E-ENS	E-HSW	14	19	31,4	0	-201.03
E-ENS	E-LLS	14	21	20	230,7193756	407.75
E-ENS	E-OHK	14	26	43,4	-242,2953606	-329.94
E-GER	E-RIL	16	28	60,3	-936,6094208	-936.6
E-GER	E-TIL	16	31	24	1429,780884	1606.9
E-HGL	E-GRO	18	17	16,5	0	0
E-HGL	E-ZWO	18	38	60,7	-1215,81398	-1038.5
E-HSW	E-ZYV	19	39	63,9	-375,5255508	-576.53
E-KIJ	E-BWK	20	6	17,5	-378,0908585	186.53
E-KIJ	E-GER	20	16	34	51,19315147	228.25
E-LLS	E-DIM	21	9	51,7	133,3525658	310.45
E-LSM	E-BGM	22	1	10,9	-524,1004944	-611.74
E-MBT	E-BMR	23	3	58	0	177.25
E-MBT	E-EYC	23	15	8,5	0	0
E-MBT	E-SIE	23	29	10,6	0	0
E-MEE	E-DIE	24	8	17	0	0
E-MEE	E-ZWO	24	38	107,8	1215,81398	926.83
E-MVL	E-SMH	25	30	23	340,9243774	1082.5
E-OHK	E-LSM	26	22	28,5	-370,1696396	-457.74
E-OZN	E-DIM	27	9	15,5	673,5019684	496.35
E-RIL	E-BSL	28	4	39,1	-1149,010391	-1149
E-RIL	E-ZAN	28	37	6,5	0	0
E-SMH	E-CST	30	7	43	144,8987484	886.48
E-TIL	E-EHV	31	13	40	1148,596344	1325.8
E-VHZ	E-BVW	32	5	15	-87,38775253	-264.45
E-BWK	E-VHZ	6	32	45	307,7701378	130.75
E-VVL	E-EEM	33	12	39,9	-1210,58075	-1499.6
E-WES	E-MVL	34	25	20,2	-3066,611023	-2325
E-WEW	E-MEE	35	24	29,3	270,6101418	501.13
E-WTR	E-WES	36	34	6,8	-2372,379608	-1630.8
E-ZWO	E-ENS	38	14	31,7	0	-111.72
E-ZYV	E-VVL	39	33	23,7	-375,9260178	-576.83

Table D.2: Nodes of the hydrogen component with entries and exits in INT 1039

Node	Index	Entries	Exits
H-APP	1	425,8	1272,9
H-BBG	2	76,8	2794,2
H-BCH	3	848,7	0
H-BEV	4	498,2	7327,3
H-BGS	5	369,9	760,9
H-BOT	6	51,3	3696,4
H-EEM	7	0	1469,3
H-EMD	8	485	0
H-EMM	9	199	460,7
H-ESV	10	88,3	1925,4
H-GRK	11	49,2	1057,9
H-GRV	12	630,4	0
H-HAR	13	124,5	853,8
H-HIL	14	1091,2	0
H-JUL	15	363,7	0
H-LLS	16	109,1	1313,5
H-MBT	17	116,4	4100,8
H-MVL	18	396,1	4374,5
H-OMM	19	508,7	2377,7
H-OSS	20	164,9	2836,2
H-OSZ	21	1188,1	0
H-RAV	22	583	4128,4
H-SDA	23	35553,4	360,8
H-WGD	24	413,2	4256,3
H-WIE	25	11,7	483
H-WIN	26	485	0
H-ZAN	27	121,2	0
H-ZEL	28	412,2	0
H-ZEV	29	485	0

Table D.3: Lines of the hydrogen component with optimal transport load in INT 1039

From	To	From index	To index	Length (km)	Flow
H-APP	H-SDA	1	23	13	0
H-BBG	H-HIL	2	14	8	-1091,2
H-BBG	H-ZAN	2	27	65	-121,2
H-BEV	H-WGD	4	24	91	0
H-BGS	H-BEV	5	4	20	6828,9
H-BOT	H-WGD	6	24	24	-7623,5
H-EEM	H-APP	7	1	15	9912,6
H-EMD	H-EEM	8	7	13	11381,8
H-EMD	H-SDA	8	23	29	-10896,9
H-EMM	H-OMM	9	19	58,8	-261,7
H-ESV	H-WIN	10	26	34,2	-485
H-ESV	H-ZEV	10	29	33,2	-485
H-GRK	H-APP	11	1	44	-9065,6
H-GRK	H-HAR	11	13	70	729,4
H-GRK	H-WIE	11	25	114	7327,6
H-WIE	H-JUL	25	15	25,5	-363,7
H-MBT	H-BCH	17	3	20	-848,7
H-MBT	H-GRV	17	12	16	-630,4
H-MVL	H-BOT	18	6	36	-3978,4
H-OMM	H-ESV	19	10	56	867,2
H-OMM	H-LLS	19	16	68,3	1204,4
H-OMM	H-RAV	19	22	113	21281,5
H-OSS	H-ZEL	20	28	39	-412,2
H-OSZ	H-SDA	21	23	23	1188,1
H-RAV	H-BBG	22	2	53	1505
H-RAV	H-MBT	22	17	120	2505,3
H-RAV	H-WGD	22	24	72	13725,9
H-SDA	H-OMM	23	19	100	25483,8
H-WGD	H-OSS	24	20	77	2259,2
H-WIE	H-BGS	25	5	24	7220

E

NETWORK PLOTS

This appendix contains the plots for instances 0834 and 4044. Appendix E shows the absolute and relative load in the hydrogen network of instance 0834. As mentioned in chapter 5, the quantities of hydrogen in the network are relatively small and the network is far from being saturated.

In appendix E, we see the absolute and relative hydrogen load for instance 4044. This time, as in case 1039, the network is dealing with larger amounts of gas and the busiest line (in relative terms) is functioning around two thirds of its capacity. This busiest line is the same as for 1039, i.e. pipe RAV-WGD. For all three instances, the largest quantity of gas passes through the same two pipes, SDA-OMM and OMM-RAV, but their capacity is large enough that they are not saturated.

Figures E.3 and E.4 show the absolute and relative load of the power network, calculated with transport load optimization, for instances 0834 and 4044 respectively. In both cases, the network appears to be loaded way beyond an acceptable state, with at least one line carrying 100% of its capacity. (Recall that the relative load in any given line should not exceed 50% for the state of the network to be considered acceptable.)

Power flows computed with the DC model are shown in fig. E.5 and fig. E.6. This time, the maximum line saturation is even over 100%, occurring in the same lines as before. Overall, the flows calculated by the two models are qualitatively close. However, we know that there is still a large difference between the two. This is visible in fig. E.7 and fig. E.8: lines with no error are shown in dark blue (this concerns only a few lines with no power flow at all), error under 10% in light blue, between 10% and 25% in bright red, and over 100% in dark red. Knowing that DC power flow is the accurate one, transport load is clearly an inadequate way to calculate power flows.

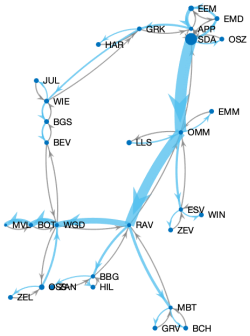

(a) Optimal transport load of hydrogen in 0834

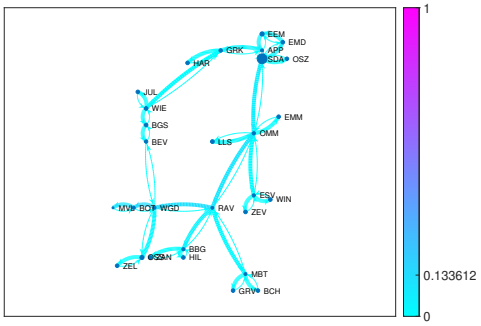

(b) Flow of hydrogen compared to pipe capacity in 0834

Figure E.1: Hydrogen flows in 0834

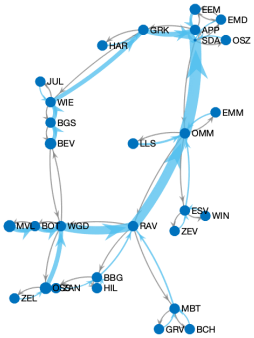

(a) Optimal transport load of hydrogen in 4044

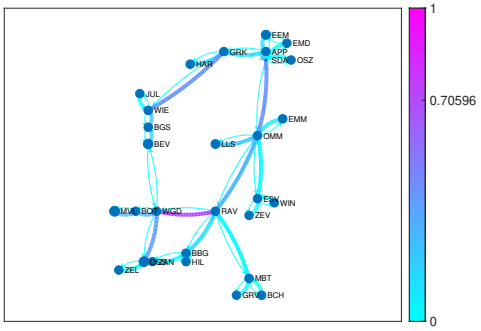

(b) Flow of hydrogen compared to pipe capacity in 4044

Figure E.2: Hydrogen flows in 4044

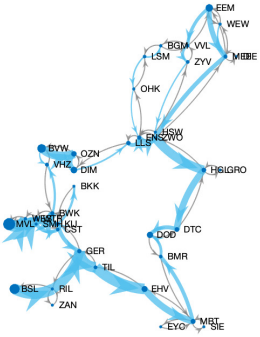

(a) Optimal transport load of power in 0834

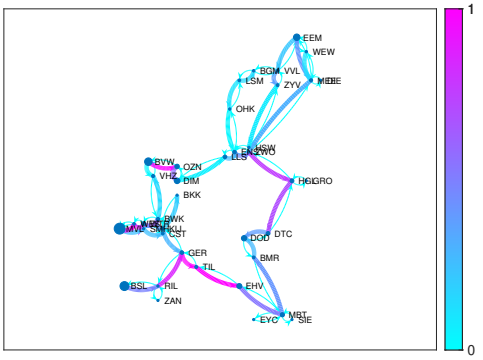

(b) Optimal transport load compared to line capacity in 0834

Figure E.3: Power transport load in 0834

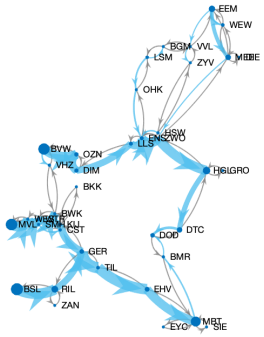

(a) Optimal transport load of power in 4044

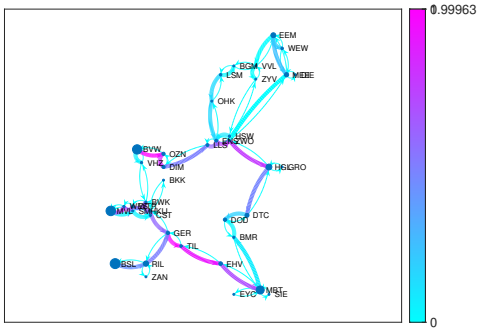

(b) Optimal transport load compared to line capacity in 4044

Figure E.4: Power transport load in 4044

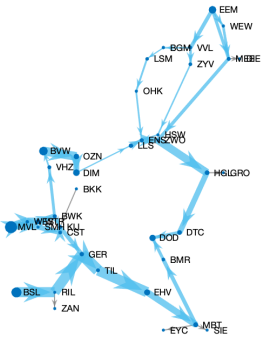

(a) DC power flow in 0834

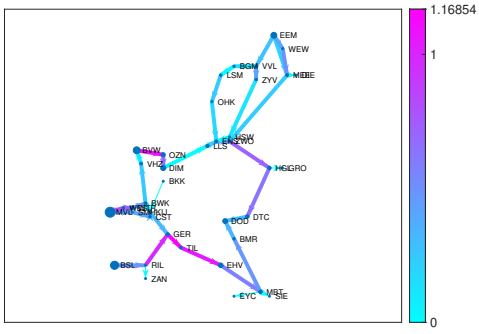

(b) DC power flow compared to line capacity in 0834

Figure E.5: DC power flows in 0834

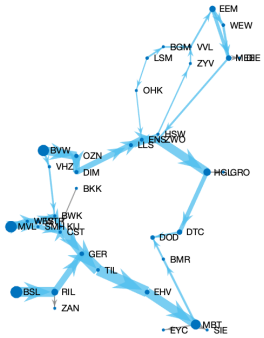

(a) DC power flow in 4044

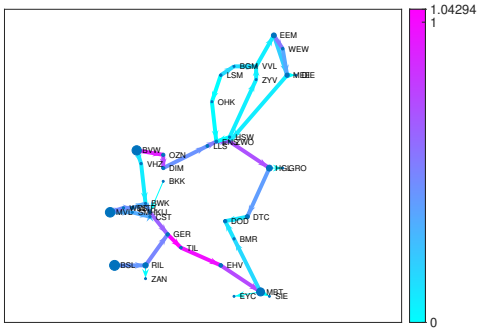

(b) DC power flow compared to line capacity in 4044

Figure E.6: DC power flows in 4044

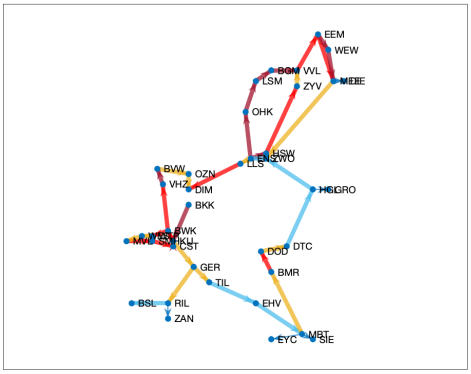

Figure E.7: Difference between power flows in 0834

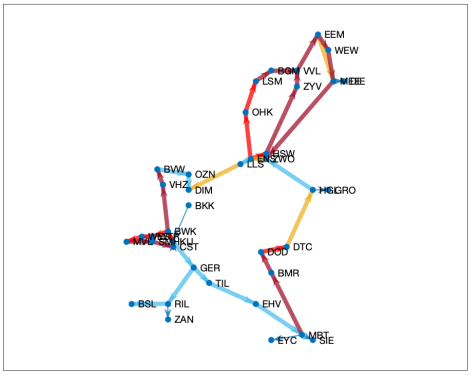

Figure E.8: Difference between power flows in 4044

F

MATLAB CODE

This appendix contains the most important pieces of code used through this project. In the first section, we give the code used to compute flows and optimal generation using the combined model. In the second, we show how the functions and script used to compute flows in the Dutch network instances.

F.1. THE COMBINED MODEL

This function computes optimal power generation and optimal gas transport load. Power flows can subsequently be computed from the resulting power generation and given power demand.

```
function [powergen, gasload, cost] = optimDCTL(network)
% OPTIMIZATION: gas transport load and DC OPF
%   INPUT: struct network containing all the input data
%
% OUTPUT:
%   powergen = the amount of power given off by each generator
%   load = the quantity of gas in each line (optimization variables)
%   cost = resulting value of the cost function

% [x, fval] = linprog(f,A,b,Aeq,beq,lb,ub)
Ngaslines = length(network.gassourcenodes);

%% Construct problem data for gas
branchnames = strcat("Q", string(1:Ngaslines));
% Branch-node connectivity matrix:
G = digraph(network.gassourcenodes, network.gastargetnodes);
connectivity = -incidence(G);
% Corresponding branch reordering:
```

```
[~, reordering] = sortpairs(network.gassourcenodes, network.
    gastargetnodes);
%branchnames = branchnames(reordering);
lengths = network.lengths(reordering);

%% Construct problem data for power
ngen = length(network.powercosts);

%% Build full problem
costs = [network.powercosts; lengths];

% inequality constraints based on PTDF
if ~isempty(network.ptdf)
   A = [network.ptdf; -network.ptdf];
   A = [A zeros(size(A, 1), Ngaslines)]; % append zeros for size
       compatibility
   ptdfwithloads = network.ptdf*network.powerdemands;
   b = [network.powerlinecaps + ptdfwithloads;
        network.powerlinecaps - ptdfwithloads];
else
    A = [];
    b = [];
end

Aeq = blkdiag(ones(1,5), connectivity);
beq = [sum(network.powerdemands); network.injections];

% Add in coupling coefficients
C = network.gfgmatrix;
for k=1:size(C,1)
    % Col 1 of C gives row, col 2 gives column, col 3 gives value
   Aeq(C(k,1), C(k,2)) = C(k,3);
   % set gas injection to 0 at the gfg coupling nodes
    beq(C(k, 1)) = 0;
end
C = network.ptgmatrix;
for k=1:size(C,1)
    % Col 1 of C gives row, col 2 gives column, col 3 gives value
   Aeq(C(k,1), C(k,2)) = C(k,3);
   % don't touch right side this time
end

%full(Aeq)
%beq

```

```
lb = [network.minpower; network.mingasload];
ub = [network.maxpower; network.maxgasload];

[x, cost] = linprog(costs,A,b,Aeq,beq,lb,ub);

powergen = x(1:ngen)';
gasload = x(ngen+1: end)';
```

F.2. DUTCH NETWORKS

The first function given here carries out the construction and solving of the optimization problem for transport load. A slightly modified version of the problem is used instead of the proper equivalent problem derived in appendix C: in the first place, all the lines are duplicated into their positive-direction and negative-direction components, each with the appropriate maximum capacity and with the minimum capacity set to zero. This is why lines are duplicated on all the transport load plots in this report. Additionally, the capacities of the lines are a hard limit. Any excess flow is directed into extra lines with very high cost. This mimics the piecewise-linear problem of transport load optimization.

Also note the reordering of the lines. In order to obtain the incidence matrix of the network, which is needed for the equality constraints, the graph of the network is generated using the lists of source and target nodes of the edges. The resulting list of edges is sorted in ascending order of these pairs. For example, if the source nodes are (1,2,1) and the target nodes are (3,1,2), the corresponding pairs are ((1,3), (2,1), (1,2)). In ascending order, this list becomes ((1,2), (1,3), (2,1)). All the data associated with branches (i.e., the lengths and capacities) needs to be reordered accordingly. The list of flows resulting from the optimization step is also in this order. As the last step of the function, it is restored back to its original order to avoid confusion.

```
function pwgasload = tlopt(source, target, mincap, maxcap, inj,
    lengths)
% OPTIMIZATION: gas transport load coupled to a known power network
% PSeudo-piecewise linear programming
%   INPUT: source nodes, target nodes, minimum capacity (in fact 0),
%   maximum capacity, net injection at each node, line lengths
%
% This assumes that lines have already been split into their positive
    -direction
% and negative-direction components. This is why the min capacity is
    0.
%
% OUTPUT:
%   load = the quantity of gas in each line (optimization variables)
%   cost = resulting value of the cost function

%% Construct problem data for gas
Nlines = length(source);
```

```
Nnodes = length(inj);

% Mimic piecewise linear programming by adding extra lines that can
    absorb overflow
% Branch-node connectivity matrix:
totalfrom = [source; source];
totalto = [target; target];
G = digraph(totalfrom, totalto);
C = -incidence(G);
% Corresponding branch reordering:
[~, reordering] = sortpairs(totalfrom, totalto);

% set costs of extra lines very high
linecosts = [lengths; 1e6*ones(Nlines, 1)];
linecosts = linecosts(reordering);

% Lower and upper bound
lb = [mincap; mincap];
ub = [maxcap; 10*maxcap];

lb = lb(reordering);
ub = ub(reordering);

% [x, fval] = linprog(f,A,b,Aeq,beq,lb,ub)
% [gasload, cost] = linprog(lengths, [], [], connectivity, inj,...
  %                               mincap, maxcap);

%% build optimization problem
% relaxed version
A = [C;
    -C];
eps = 1e-6*ones(Nnodes,1);
b = [inj+eps;
    -(inj - eps)];

inversepermutation(reordering) = 1:length(reordering);
[pwgasload, pwcost] = linprog(linecosts, A,b, [], [], lb, ub);

% Reverse the reordering of the lines
pwgasload = pwgasload(inversepermutation);
end
```

Next, we have the computation of the DC power flows based on provided input and outputs of power at nodes. This function uses calculations described in appendix A. It also involves reordering of the lines.

```
function flow = dcflow(from, to, lengths, inj)
%Pinj = Bbus delta (phase angles), solve for delta
% then Pline = Bline delta

% make graph
G = digraph(from, to);
M = incidence(G);

% reorder rows accordingly
[~, reordering] = sortpairs(from, to);
inversepermutation(reordering) = 1:length(reordering);

b = 4./lengths(reordering);

% Compute line susceptance and bus susceptance matrices
Bline = -diag(b)*M';
Bbus = -M*Bline;

% Cholesky decomposition of Bbus (helps with condition number)
R = chol(Bbus); % upper triangular

% Au=f, A=LU then solve Ly=f and Uu=y
% Here L = R'
y = R'\inj;
delta = R\y;

flow = Bline * delta;
flow = flow(inversepermutation);

end
```

Finally, a script sets up the calculations and and calls the above two functions. The structure `network` contains data read from an excel file that contains the instance data.

```
% OPTIMIZATION: gas transport load coupled to a known power network
% Pseudo-piecewise linear programming
%   INPUT: struct network containing all the input data
%
% OUTPUT:
%   branches, an array of string arrays containing branch names properly
%       reordered for each network
%   dcpf, the power flow obrained using ptdf of the network
%   powercapreached = 0 if dcpf is under capacity for the whole network,
%                   = 1 otherwise
%   halfcapreached: the same but checking whether dcpf is under one half of
%       the line capacity
%   powertl: flows in power network computed using transport load
%   hload: TL in hydrogen network
%   gload: TL in natgas network

%%
sourcenodes = network.powersourcenodes(1:43);
targetnodes = network.powertargetnodes(1:43);
len = network.powerlinelengths(1:43);
inj = (network.powerentries - network.powerexits);

dcpf = dcflow(sourcenodes, targetnodes, len, inj);

%% compute optimal transport load for both networks
powertl = tlopt(network.powersourcenodes, network.powertargetnodes, ...
                zeros(size(network.maxpowerload)), network.maxpowerload,...
                network.powerentries-network.powerexits, network.powerlinelengths);
% add together the power in the regular lines and the extra ones
powertl=powertl(1:86)+powertl(87:172);

hydrogentl= tlopt(network.hsourcenodes, network.htargetnodes, ...
                  network.minhload, network.maxhload,...
                  network.hinjections, network.hlengths);
hydrogentl=hydrogentl(1:60)+hydrogentl(61:120);
```